Zhu *et al. Soft Sci* 2024;4:17
DOI: 10.20517/ss.2024.05

Soft Science

Review Article

Open Access

Check for updates

Latest developments and trends in electronic skin devices

Pengyu Zhu[1], Zihan Li[1], Jinbo Pang[2,*], Peng He[1,*], Shuye Zhang[1,*]

[1]State Key Laboratory of Advanced Welding and Joining, Harbin Institute of Technology, Harbin 150001, Heilongjiang, China.
[2]Institute for Advanced Interdisciplinary Research (iAIR), University of Jinan, Jinan 250022, Shandong, China.

[*]**Correspondence to:** Prof. Jinbo Pang, Institute for Advanced Interdisciplinary Research (iAIR), University of Jinan, 336 Nanxinzhuang West Road, Jinan 250022, Shandong, China. E-mail: jinbo.pang@hotmail.com; Prof. Peng He, Assoc. Prof. Shuye Zhang, State Key Laboratory of Advanced Welding and Joining, School of Materials Science and Engineering, Harbin Institute of Technology, 92 Xidazhi Street, Nangang District, Harbin 150001, Heilongjiang, China. E-mail: nanojoin@hit.edu.cn; syzhang@hit.edu.cn

How to cite this article: Zhu P, Li Z, Pang J, He P, Zhang S. Latest developments and trends in electronic skin devices. *Soft Sci* 2024;4:17. https://dx.doi.org/10.20517/ss.2024.05

Received: 31 Jan 2024 **First Decision:** 8 Mar 2024 **Revised:** 2 Apr 2024 **Accepted:** 16 Apr 2024 **Published:** 14 May 2024

Academic Editors: Sang Min Won, Zhifeng Ren **Copy Editor:** Dong-Li Li **Production Editor:** Dong-Li Li

Abstract

The skin, a vital medium for human-environment communication, stands as an indispensable and pivotal element in the realms of both production and daily life. As the landscape of science and technology undergoes gradual evolution and the demand for seamless human-machine interfaces continues to surge, an escalating need emerges for a counterpart to our biological skin - electronic skins (e-skins). Achieving high-performance sensing capabilities comparable to our skin has consistently posed a formidable challenge. In this article, we systematically outline fundamental strategies enabling e-skins with capabilities including strain sensing, pressure sensing, shear sensing, temperature sensing, humidity sensing, and self-healing. Subsequently, complex e-skin systems and current major applications were briefly introduced. We conclude by envisioning the future trajectory, anticipating continued advancements and transformative innovations shaping the dynamic landscape of e-skin technology. This article provides a profound insight into the current state of e-skins, potentially inspiring scholars to explore new possibilities.

Keywords: Electronic skin, sensor, human-machine interface, multimodal, machine learning

INTRODUCTION

The skin, the largest organ in the human body, serves not only as a physical protective barrier but also plays a crucial role in perceiving the external environment, regulating physiological functions, and actively participating in immune defense. Throughout the development of human work and life, the skin holds immense significance, forming the fundamental basis for human perception of the surrounding environment[1,2].

Simultaneously, the advancement of human civilization sees a notable trend in integrating intelligent machinery, robots, and manufacturing into our daily lives, ushering in a significant transformation toward the digitization and intelligence of various aspects of human existence. These elements are intricately interconnected, collectively driving a profound change in society[3].

The increasing need for Human-Machine Interfaces (HMI) has led to a notable trend in replicating the sensory capabilities of human skin, facilitated by advancements in electronics and materials science[4-6]. Referred to as electronic skins (e-skins), this innovation holds substantial potential across various domains such as flexible wearable electronics, health monitoring, healthcare, robotics, smart manufacturing, smart homes, and more[7,8].

An electronic skin (e-skin) system needs to possess the following basic characteristics:

First, akin to human skin, e-skins should be flexible, stretchable and tough enough. They need to adapt well to the movement of the torso, machinery, or devices in applications while preserving their sensing function, and thus, some stretchable structures need to be developed to maintain the sensing capability of the active devices[9]. Obviously, flexible stretchable materials are an important foundation; materials such as hydrogel, cellulose, and polydimethylsiloxane (PDMS) are widely used[10-12].

Second, resembling human skin, e-skins need to be carefully designed to provide various sensing capabilities. Examples include the ability to sense stimuli such as strain[13-15], temperature[16,17], and humidity[18-21].

Thirdly, similar to human skin, e-skins should also have good self-healing ability. To better cope with the complex environment, they may face too strong stimuli, which will significantly extend their lifespan[22,23].

Fourth, the e-skins applied in some special scenarios should have certain specific characteristics, such as biocompatibility, self-supply of energy, energy storage, transparency, color-changing capabilities, cold resistance, recyclability, biodegradability, and so on.

Taking a broad perspective, a human skin system involves the coordinated operation of various subsystems, including the skin itself, the brain and nervous system, and the heart and blood circulation system. Similarly, an e-skin system comprises three essential subsystems: a sensor subsystem emulating the functions of human skin, a signal collection/transmission/processing subsystem mimicking the roles of the brain and nervous system, and an energy supply subsystem replicating the functions of the heart and blood circulation.

Within this framework, the sensor system is tasked with detecting pertinent external stimuli or physiological signals and transforming them into measurable electrical signals. The signal collection/

transmission/processing system, on the other hand, gathers signals from the sensor system and subsequently transmits and processes them. Lastly, the energy supply system plays a critical role in providing power to these subsystems, with energy collection and supply mechanisms encompassing options such as batteries, triboelectric devices, and piezoelectric devices[24].

Evidently, the sensor system constitutes the foundation of the entire system. The construction of a perceptual capability that is clear and precise across various stimuli stands as a pivotal element in developing an ideal e-skin and, consequently, intelligent systems built upon it. On this basis, multimodal e-skins with multiple sensing capabilities and e-skin systems empowered with internet of things (IoT) integration and machine learning (ML) approaches are more capable of meeting the needs in practical applications. The development of e-skins has been accelerating in recent years, and they are bound to become an integral part of people's lives. Therefore, it becomes imperative to curate and analyze the latest progress in the field of e-skins.

While several notable scholars have previously provided excellent reviews and commentaries on e-skins[25-28], the domain has experienced rapid evolution, necessitating a comprehensive consideration of recent emerging research. This entails a reevaluation of the current state of research and a forward-looking perspective toward future developments.

This paper aims to integrate and summarize the strategies and research progress of e-skins. Firstly, we take stock of several basic capabilities and the main implementation strategies of e-skins, which include strain sensing, pressure sensing, shear force sensing, temperature sensing, humidity sensing, and self-healing capability. Subsequently, we will briefly introduce complex e-skin systems and current major applications [Figure 1] to facilitate readers to swiftly grasp advancements in this field. Finally, we will delve into discussions regarding existing challenges and potential future directions. We hope this review article serves as a wellspring of inspiration, assisting readers in forging their pursuits in this emerging research domain.

BASIC SENSING CAPABILITIES OF E-SKINS

The basic sensory capabilities of human skin include five aspects: strain, pressure, shear, temperature, and humidity, of which the combined perception of strain, pressure, and shear constitutes the "tactility". In addition, human skin can heal itself in response to overpowering stimuli.

The basic implementation strategy of e-skins to perceive these stimuli is to utilize the established physical ground stimulus-response law to design the conductive pathway and structure of the flexible device to achieve the mapping between the external stimulus and the change of the electrical signals in the conductive pathway, and to realize the perception of the corresponding stimulus through the detection of the electrical signals collected by computer. These signals include resistance[29-31], capacitance[32,33], piezoelectricity, semiconductor properties, triboelectricity, and so on.

In this section, we will present the basic implementation strategies and representative works of existing e-skin systems.

Pressure sensing capability

There are four main categories of pressure sensors: (1) piezoresistive; (2) capacitive; (3) piezoelectric; (4) triboelectric[34-36] [Figure 2A].

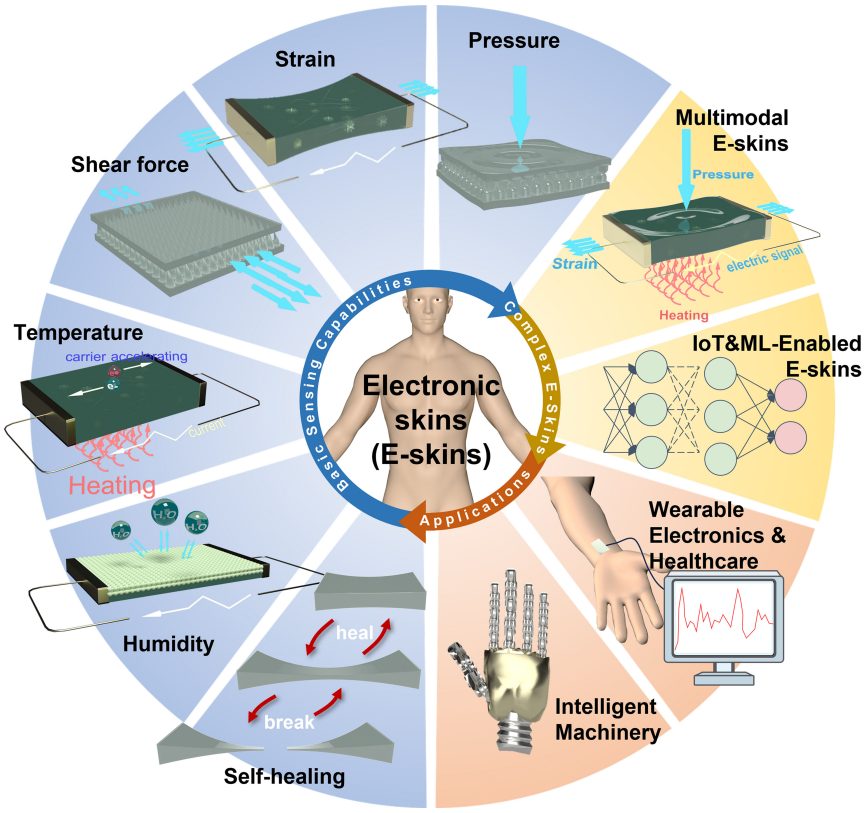

Figure 1. Overview of electronic skins, including the aspects (basic sensing capabilities, complex e-skins, applications) that are vital to their design. IoT: Internet of things; ML: machine learning.

(1) Piezoresistive conductive composite pressure sensors consist of a stretchable elastomer and conductive fillers, and the resistance of the sensor varies with the compressive strain of the device, sensing the external compressive stress based on its piezoresistivity[37-40]. This basic principle not only works during material compression but also during tensile strain, so some strain sensors also possess a certain degree of pressure sensing capability[40].

Scholars often enhance their performance further through special designs such as multilayers[41,42], patterned conductive paths[43], and bionics[44], which require novel geometrical designs of sensor structures.

Sencadas *et al.* demonstrated a biodegradable porous piezoresistive sensor (MWCNT-PGS) made of poly(glycerol sebacate) (PGS) blended with multi-walled carbon nanotubes (MWCNTs) for real-time monitoring complex human movements, and the prepared sensor can be degraded by water[45]. The unique porous properties enhance its performance [Figure 2B], and it exhibits high reliability, long lifetime (> 200,000 cycles), short response time (≤ 20 ms), and high force sensitivity (≤ 4 mN).

Inspired by the interlocking microstructure of the epidermal-dermal ridge of human skin, Park *et al.* developed a piezoresistive interlocked microdome array structure, providing a significant advantage over ordinary planar structure pressure sensors[46,47] [Figure 2C]. This array structure was demonstrated to be highly sensitive to detecting various mechanical stimuli, including normal, shear, tensile, bending and twisting forces. This layered interlocking structure can effectively concentrate the compressive stress near the ridge tips, leading to the deformation of microstructures such as microspheres, and because the contact

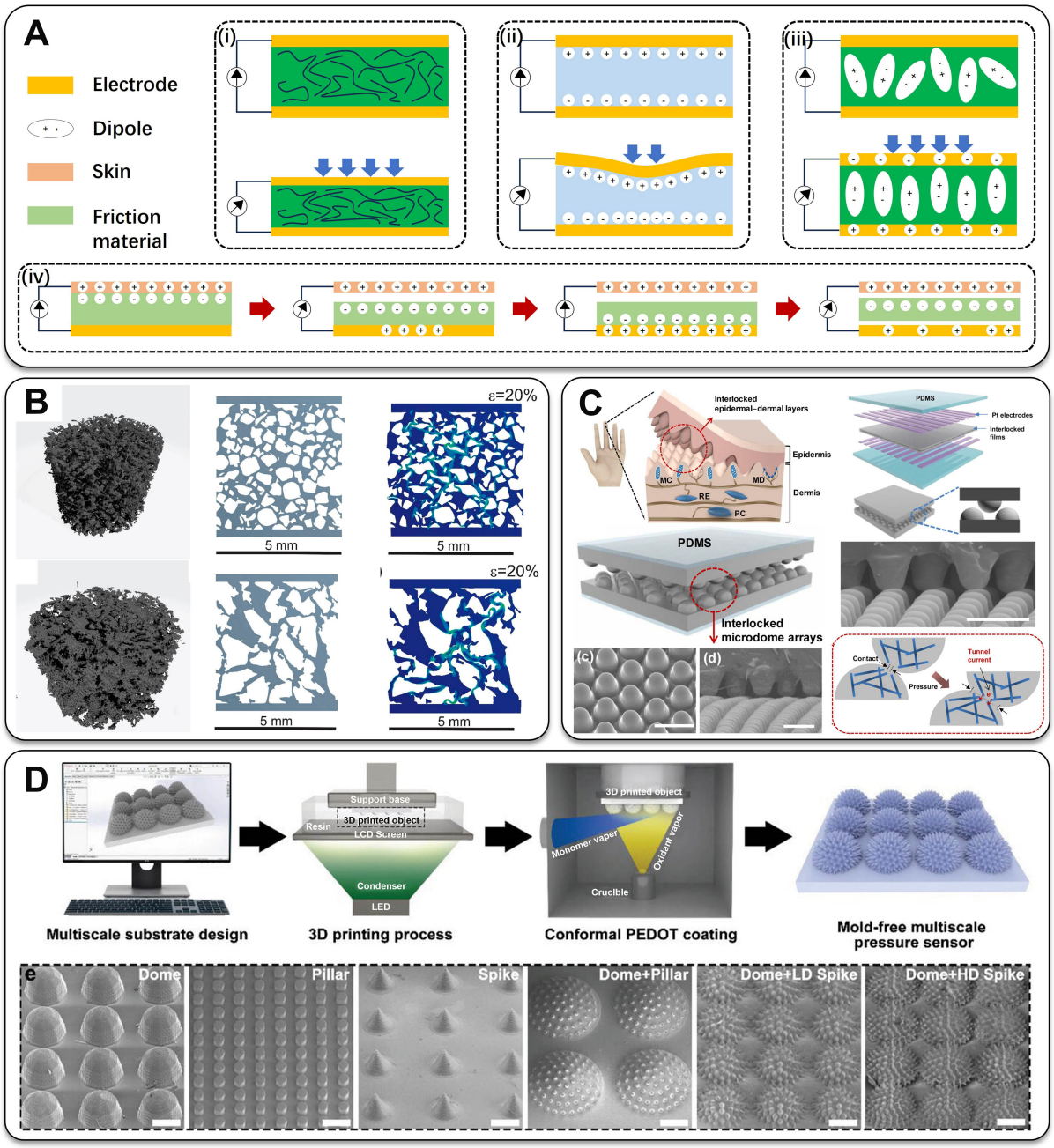

Figure 2. (A) Schematic diagram of common pressure sensing mechanisms: (i) resistive, (ii) capacitive, (iii) piezoelectric, (iv) triboelectric; (B) the microstructure and sensing mechanism of porous MWCNT-PGS sensors[45]; (C) the structure, performance, sensing mechanism of piezoresistive sensors with interlocking microsphere array interlocked microdome arrays structure[46,47]; (D) the preparation process and microstructure of the multi-scale dome/spire + stepped structure pressure sensor[51]. MWCNT-PGS: A biodegradable porous piezoresistive sensor; PDMS: polydimethylsiloxane; PEDOT: poly(3,4-ethylenedioxythiophene).

area between the specially shaped interlocking arrays can be rapidly increased, the pressure sensors of this structure possess higher performance as pressure sensors in low-pressure states[48]. Not only pressure sensing, sensors with this structure also perform well in other sensing fields such as strain, shear force, bending, and torsion[49,50].

Baek *et al.* demonstrated a maskless method for fabricating flexible pressure sensors through high-precision 3D printing and thin-film coatings of conductive polymers, which can be used to create very precise microstructures[51]. The team demonstrated diverse pressure sensors with complex multi-scale dome/spike + step-like structures, showing extremely high process controllability [Figure 2D]. The prefabricated pressure sensors presented in this work exhibit very sensitive responsiveness (up to 185 kPa^{-1}) and ultra-fast response times (≈ 36 μs), which could be utilized in smart mechanical devices.

(2) Capacitive pressure sensors operate by converting external pressure into a capacitive signal. The capacitance of a medium is known to be defined as:

$$C = \frac{(\varepsilon A)}{d}$$

where ε is the dielectric constant, A is the area of the device, and d is the distance between two conductive plates, and thus the pressure-induced changes in d and A can be used to measure the applied pressure[34,52]. Piezo-capacitive pressure sensors typically have the advantage of high sensitivity and no inherent temperature sensitivity compared to resistive pressure sensors[53-55].

It should be noted that using microstructural design to improve device performance is not exclusive to piezoresistive conductive composite pressure sensors[56-58]. Tee *et al.* prepared a pyramid-structured capacitive pressure sensor using PDMS material and investigated the compressibility of the PDMS microstructures and the effect of spatial arrangement on the mechanical sensitivity of the microstructured film[59]. It was used as a parallel plate capacitor structure in pressure sensors. The sensors showed potential for applications such as blood pulse monitoring and force-sensing touch panels.

Niu *et al.* present a facile technique based on a simple melt infiltration process and a commercial cone-shaped nanoporous anodic aluminum oxide (AAO) transfer method for large-scale and low-cost preparation of interlocking asymmetric nanocones on poly(vinylidenefluoride-co-trifluoroethylene) [P(VDF-TrFE)] films[60] [Figure 3A][60-62]. The developed capacitive tactile sensors have excellent performance, including a sensitivity of 6.583 kPa^{-1} in the low-pressure region (0-100 Pa), a detection limit as low as ≈ 3 Pa, response/recovery times as low as 48/36 ms, and excellent stability and reproducibility (10,000 cycles).

(3) Triboelectric pressure sensors utilize the triboelectric nanogenerator (TENG) triboelectric effect and the principle of electrostatic induction to detect pressure changes. In normal operation, this sensor usually contains two or more material layers inside; when subjected to pressure, these layers contact each other and move in the mechanical stress of spontaneous charge separation to generate electrostatic charge. The external pressure stimulus can produce different characteristics of the electrical signal, the contact area, the degree of contact tightness and relative sliding distance, and other factors will affect the characteristics of the generated charge; therefore, by detecting the electrical signal changes, triboelectric pressure sensors can indirectly measure the size of the applied pressure on the sensor. These sensors are self-powered and are suitable for the development of self-powered e-skins[63-66].

It has been reported that designing microstructures on the dielectric surface to provide a larger contact area and more active sites to transfer electrostatic charges during contact electrification can enhance the triboelectric effect. Yao *et al.* developed a self-powered TENG e-skin sensor mimicking a conical array of interlocking microstructures on the surface of a plant [Figure 3B], an interlocking microstructure that

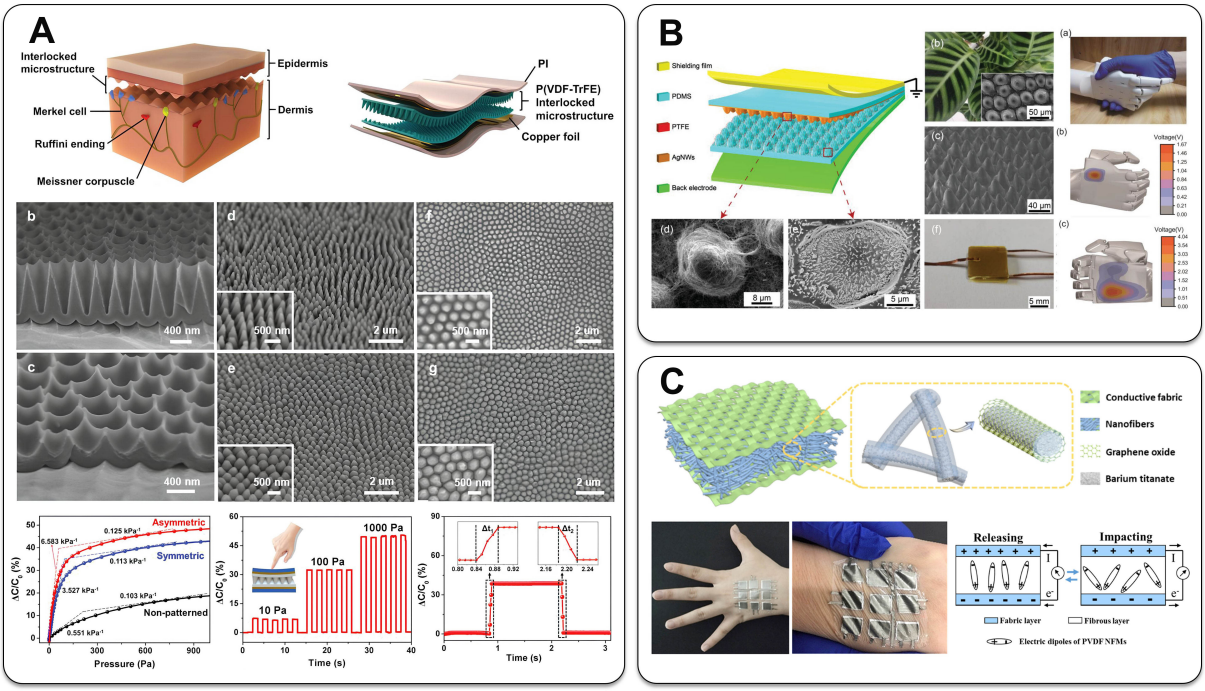

Figure 3. (A) the micro-vertebral structure and basic properties of the P(VDF-TrFE) sensor[60]; (B) the morphology of a conical array of interlaced microstructures that mimic the surface of a plant and the analysis of the sensing array on the stress distribution during a handshake[61]; (C) the piezoelectric fiber structure and sensor device characteristics[62]. PI: Polyimide; P(VDF-TrFE): poly(vinylidenefluoride-co-trifluoroethylene); PDMS: polydimethylsiloxane; PTFE: polytetrafluoroethylene; AgNWs: silver nanowires; PVDF: polyvinylidene fluoride; NFMs: nanostructured functional materials.

enhances the triboelectric effect[61]. Small polytetrafluoroethylene (PTFE) spines on the friction surface increased the sensitivity of the pressure measurement by a factor of 14. The sensor exhibits very regular and stable sensing properties, and characterization of the pressure distribution during a handshake was achieved by fabricating an array of sensors.

(4) Piezoelectric pressure sensors work by utilizing the piezoelectric effect of materials. When pressure is applied to the sensor, the piezoelectric element generates a charge signal proportional to the pressure, and this weak electrical signal is then amplified and processed by electronic circuits to reflect the pressure. Piezoelectric pressure sensors can likewise be used to create self-powered e-skins[35,67].

Out of the pursuit of smart textiles, a popular strategy is to make fibers with high piezoelectricity[68-70]. We consider that this is, at the same time, conducive to improving the contact area and obtaining better self-powered capability and signal quality[71].

Zhu *et al.* fabricated an e-skin based on coaxial piezoelectric fibers [nanofibers (NFs)] using electrostatic spinning technology, and the final piezoelectric properties of the NFs were greatly enhanced by introducing inorganic barium titanate nanoparticles (BTO NPs) with high piezoelectricity and graphene oxide (GO) nanosheets into the fibers[62] [Figure 3C]. Subsequently, a three-layer structured e-skin was made using elastic polyurethane (PU) film as the substrate and conductive fabric as the electrodes. A good sensitivity (10.89 ± 0.5 mV·kPa^{-1} in the pressure range of 80-230 kPa) and stability were demonstrated.

Huang *et al.* prepared polyvinylidene fluoride (PVDF)/carbon nanotubes (CNTs) incorporated into polyacrylonitrile/CNTs [PVDF/CNT_X@PAN/CNT_X ($DPCPC_X$)] single-layer binary fiber nanocomposite membranes (SBFNMs) using the co-electrospinning method and fabricated the interpenetrating structures of PVDF@CNT and PAN@CNT nanofiber interpenetrating structures by adding CNTs[72]. The prepared monolayer fabrics possess excellent self-powered capability and exhibit excellent synergistic effects of piezoelectricity and triboelectricity, while the triboelectric conversion is realized by the friction between the binary fibers within the membrane [Figure 4A-D]. The drawbacks of traditional piezoelectric materials are avoided, and significantly higher piezoelectric capabilities are realized.

Strain sensing capability

Due to the limitations of the underlying principles, capacitive and triboelectric principles are unsuitable for strain sensors, and strain sensors of the relevant principles tend to exhibit unfavorable performance with low sensitivity[73], with resistive strain sensors (RSSs) being the mainstream.

The sensing mechanism of RSSs utilizes the deformation of the device under the action of stress to change the structure of the conductive network inside the sensor device, thus causing corresponding changes to convey the strain information. The characteristics of the conductive network as a function of strain are the core of this type of sensor.

RSSs measure strain by analyzing the relationship between strain and resistance based on the principle that deformation of the material under stress leads to regular changes in the microscopic conductive mechanisms such as crack expansion-repair, fracture, and tunneling effects of the conductive network within the material, resulting in a corresponding change in the macroscopic resistance of the material[74,75].

Based on the substrate used, RSSs can be further classified into two categories: (1) flexible conductive polymer composites (FCPCs)-based; (2) conductive gel-based.

For FCPCs-based strain sensors, there are two main implementation strategies[76]:

(1) Filled-type FCPCs-based RSSs are made by randomly filling a stretchable polymer matrix with conductive fillers to make a conductive elastomer, which is combined with electrodes at both ends to form a tensile strain sensor[77]. Changes in the conductive network cause changes in the resistance signal during stretching, and the strain can be detected based on the correspondence therein[78]. It is favorable for sensing in a large dynamic range and also has the advantages of low cost and simple process[79]. In addition, scholars have begun to consider using sophisticated structural design to further improve performance, such as micro-cracks and micro-contacts[80,81].

Na *et al.* designed highly durable and recyclable PDMS/vertical graphene (VG)-structured RSSs with ultra-sensitive sensing properties [Figure 5A][82-84], which present a gauge factor (GF) of over 5,000 with only a very small hysteresis and maintained a stable performance after more than 10,000 cycles[82]. This study fully demonstrates that prefabricated cracks in the cluster network structure possess highly reversible resistance changes, especially after the current path is broken and the state can still be restored.

Qiao *et al.* reported total graphene artwork strain sensors (TGASSs) based on a laser engraving technique that allows the sensor to be conveniently transferred to any other surface[83]. The sensor exhibits excellent performance, including ultra-high sensitivity of up to 673 and a strain range of up to 10% with better stability, and its performance can also be adjusted by tweaking the pattern. It can be used to detect weak physiological signals such as pulse, breathing and sound [Figure 5B].

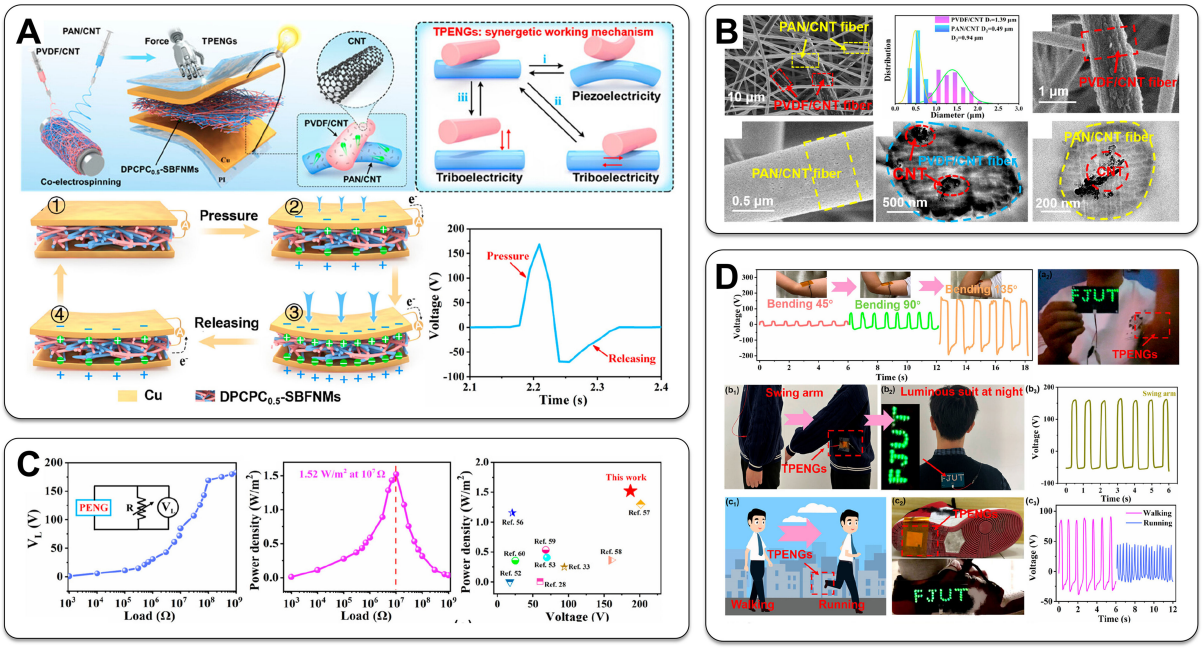

Figure 4. (A) The device structure, synergistic effect and pressure sensing mechanism; (B) structures of PVDF@CNT and PAN@CNT nanofibers; (C) excellent self-powered capability; (D) hypothetical applications of SBFNMs in self-powered wearable electronic devices[72]. PVDF@CNT: Combination of polyvinylidene fluoride (PVDF) with carbon nanotubes (CNTs); PAN@CNT: combination of polyacrylonitrile (PAN) with carbon nanotubes (CNTs).

(2) Sandwich-type FCPCs-based RSSs. Sandwich-type FCPCs-based RSSs are assembled by making a separate conductive layer of conductive material and then sandwiching it between two layers of stretchable film to form a sandwich structure to form a strain sensor[85-87].

The preparation methods of the conductive layer include deposition, spraying, transfer, coating, printing, *etc*. Due to the rapid evaporation of organic solvents during the preparation of the conductive layer, an extremely large number of microcracks are usually present on the conductive layer. When the sensor is stretched, the microcracks expand, resulting in a degradation of the conductivity of the entire device and an increase in sensor resistance. When the tension is released, the microcracks recover, allowing the conductive channel to recover and the sensor resistance to decrease. Since the crack gap increases significantly with strain, crack-type strain sensors are extremely sensitive to weak strain stimuli and also facilitate a lower detection limit[88]. Therefore, many works tend to pre-stretch the substrate when preparing the conductive layer in order to produce more crack structures[81]. Chen *et al.* fabricated an innovative PDMS/graphene/PDMS sensor with a more stable sensing network prepared by a one-step solvent evaporation method and an extended temperature monitoring range[84]. The prepared sensor exhibited resistivity dependence on temperature and strain variations [Figure 5C], with temperature and strain monitoring resolutions of 0.5 °C and 0.0625%, respectively, and excellent reproducibility.

Gel-type materials comprise a polymer network and a solution containing a large number of ions and have remarkable flexibility, excellent adhesion to the skin, and strong biocompatibility, making them ideal candidates for the manufacture of sensors and devices that can be attached to the human body or even implanted[89-92]. Based on the material system of polymer networks + ionic solutions, they can be classified into three main categories: hydrogels, organogels, and organohydrogels[93] [Figure 6A].

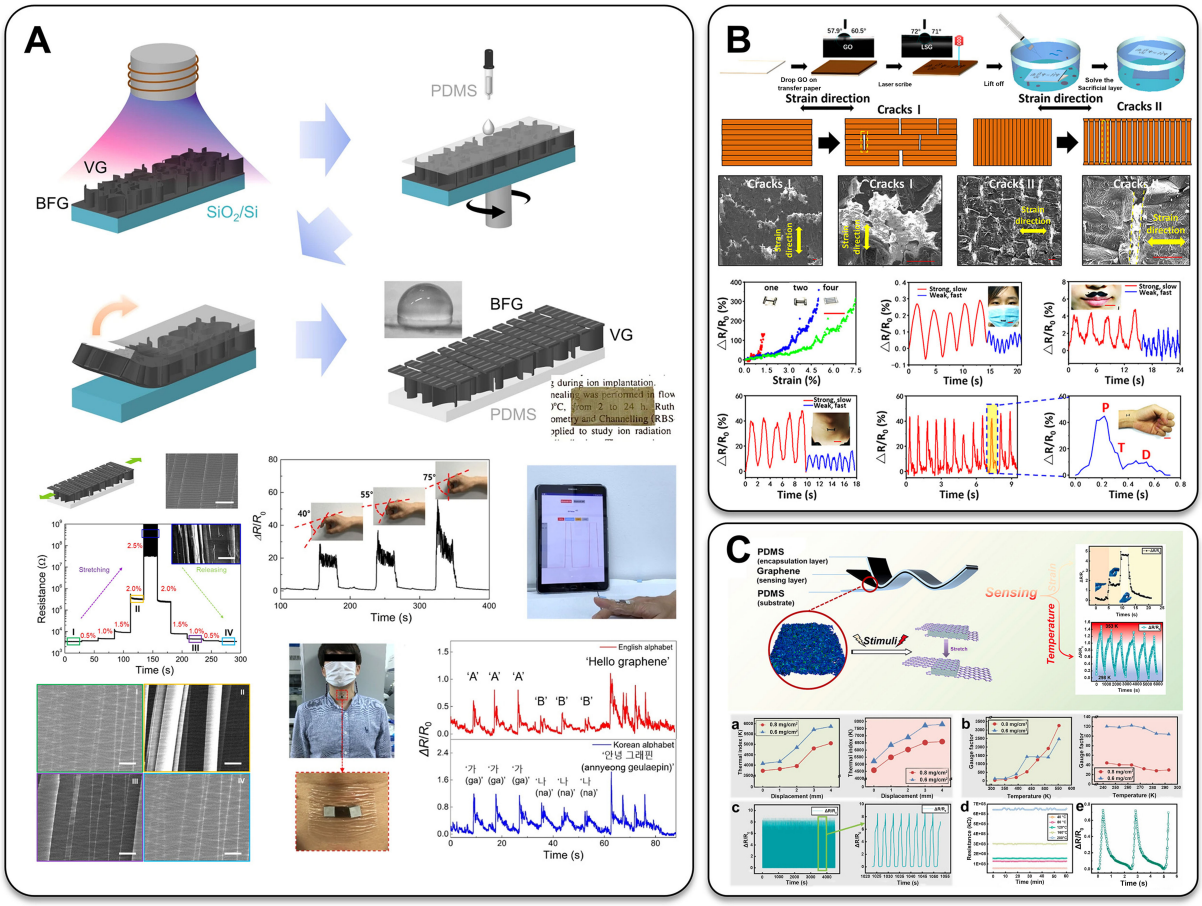

Figure 5. (A) Schematic diagram of the preparation process, structure, performance and application scenario of the PDMS/VG sensor[82]; (B) the preparation process, structure, sensing mechanism and performance of TGASSs[83]; (C) the structure and performance of the PDMS/graphene/PDMS sensor[84]. BFG: buffer flat graphene; VG: vertical graphene; PDMS: polydimethylsiloxane; TGASSs: total graphene artwork strain sensors.

Xie *et al.* prepared Chitosan/poly(acrylic acid-co-acrylamide)/MXene@polyethyleneimine [CS/P(AA-co-AAm)/MXene@PEI]/Fe^{3+}+Cu^{2+} nanocomposite bi-network hydrogels by thermal cross-linking, which exhibited excellent properties (including 2.64 MPa tensile strength, 689% elongation at break, 10.25 $MJ·m^{-3}$ toughness and 1.89 $S·m^{-1}$ conductivity)[94]. Sensors made with this hydrogel can achieve linear sensing over a strain amplitude of more than 300%, showing excellent potential for diverse applications [Figure 6B]. Lei *et al.* reported a dual-responsive multifunctional ion-conducting hydrogel [sodium dodecyl sulfate-incorporated poly(acrylamide) hydrogel (SN-PAAM)] that is dual-stimulated to temperature/strain, with an elongation of 1,836% and a response time of only 120 to 130 ms[95]. In addition, the introduction of the thermal phase change unit of sodium dodecyl sulfate (SDS) allows it to undergo a phase change at different temperatures, with an opaque/transparent transition within ten seconds when the temperature changes [Figure 6C].

Although ionic hydrogel-based strain sensors have the advantages of good flexibility, biocompatibility, and excellent strain sensing performance, their environmental stability has been an intractable problem due to the volatilization, evaporation, and coagulation of the aqueous solvents in the hydrogel, limiting their

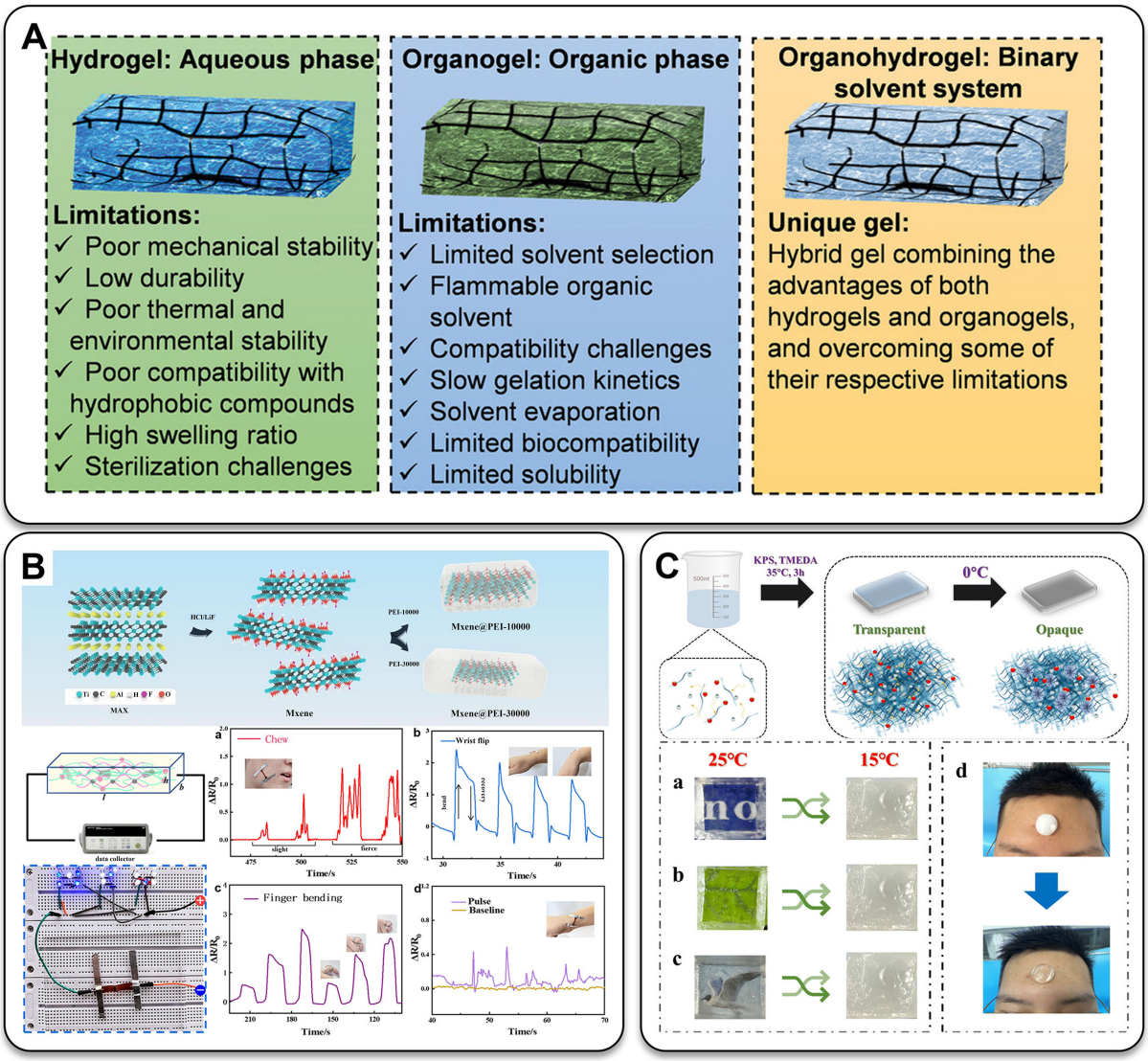

Figure 6. (A) Various gel materials and their characteristics[93]; (B) Schematic structure and main properties of CS/P(AA-co-AAm)/MXene@PEI/Fe^{3+}+Cu^{2+} nanocomposite dual network hydrogel[94]; (C) the opaque/transparent transition of SN-PAAM dual-responsive ion-conducting hydrogel[95]. KPS: Potassium persulfate; TMEDA: tetramethylethylenediamine; CS/P(AA-co-AAm)/MXene@PEI: Chitosan/poly(acrylic acid-co-acrylamide)/MXene@polyethyleneimine; SN-PAAM: sodium dodecyl sulfate-modified poly(acrylamide) hydrogel.

application areas[96]. Some application scenarios require hydrophobicity[97]. Organo-hydrogel- and ionogel-based strain sensors using organic solvents can alleviate these problems and typically exhibit dominance to freezing, desiccation, and long-term stability[98-100]. Mao *et al.* developed a poly[oligo(ethylene glycol) methylacrylate-co-acrylic acid]/hydrated ionic liquid [P(OEGMA-co-AA)/HIL] hydrogel with good electrical conductivity, self-healing ability, and frost resistance by a simple *in situ* photopolymerization strategy[101]. The incorporation of ionic liquid (IL) greatly reduces the freezing point of water, which gives the sensor excellent anti-freezing properties. The temperature dependence of the abundant hydrogen bonding it contains endows this ionic hydrogel with switchable transparency, which allows for the visualization of ambient temperature, demonstrating the potential of the gel material for temperature sensing.

Shear sensing capability

The detection of shear forces by human skin does not only refer to the perception of lateral forces applied to the skin surface but also to the perception of wind and proximity[102]. The bionic micro-spine or hemispherical structures, commonly used in other sensors, can only be used to sense the magnitude of the force, not the direction of the force, and are inapplicable to the needs of shear force sensors. Sensor structures commonly used in the field of shear force sensing are fluff structures[102-104].

Yu *et al.* developed a capacitive shear force sensor with tilted micro-hair arrays (TMHAs) by mimicking the hair structure of human skin[105] [Figure 7A][105,106]. The asymmetric microhair structure dielectric layer was obtained by the two-photon polymerization (TPP) method, which would allow different deformations due to shear forces in various directions to discriminate the direction of the force. The sensor can determine the direction of static and dynamic shear forces, exhibit a large response scale from 30 Pa to 300 kPa with a relative capacitance change $\Delta C/C_0 < 2.5\%$, and maintain high stability even after 5,000 cycles.

In addition, the recognition of the direction of shear force can be realized using the strategy of multi-sensor array + array structure design + signal processing[107]. Zhu *et al.* proposed a haptic sensor based on a multi-touch mechanism using a structure of PDMS/MWCNTs with conductive and curved surfaces, which sequentially contact the resistive columns on the micro-honeycomb electrodes (MHEs) according to the pressure to maintain proper piezoresistive characteristics [Figure 7B], and the whole sensor is characterized by high sensitivity, high linearity, good robustness, and wide dynamic range[106]. By adjusting the contact distribution density and the curvature of the PDMS/MWCNTs contact, the sensitivity and detection range can be tuned (500 kPa + 64.68 kPa^{-1} for high sensitivity mode, 1,400 kPa + 25.88 kPa^{-1} for wide range mode). The possibility of realizing normal and force measurements was demonstrated by fabricating a triaxial tactile sensor capable of sensing normal force (0-3.5 N) and shear force (0-1.5 N) with sensitivities of 58.097 and 36.137 N^{-1}.

Temperature sensing capability

Temperature sensing capability provides early warning of burn/frostbite risk and is important for the skin system to maintain intact function. There are four main types of sensing mechanisms for temperature sensors: resistive[108,109], capacitive[110], piezoelectric, and triboelectric[111,112]. Resistive temperature sensors are the most common type[113,114]; their basic principle is that the resistance of the device changes with temperature due to the thermal transport/scattering mechanism of the thermosensitive material and the change in geometry with temperature[115,116]. One of the difficulties of temperature sensors is achieving a high level of resolution.

Li *et al.* prepared a PEDOT-TPU composite fiber (PTCF) temperature sensor by growing poly(3,4-ethylenedioxythiophene) (PEDOT) *in situ* on the surface of thermoplastic PU (TPU) fibers using *in situ* polymerization[117]. The sensor exhibited a sensitivity as high as 0.95% $°C^{-1}$ and a high linearity between 20 and 40 °C. Additionally, the best part is the temperature resolution of up to 0.2 °C. The temperature-sensing fibers can be easily embedded in textiles. By sewing the fibers in an S-shape into normal textiles, strain disturbances can be virtually avoided, even when the textile is stretched to 140%.

Temperature changes can lead to variations in ion mobility, so gel materials that contain a large number of ions and are predominantly ion-conductive can also be designed as temperature sensors[118-120]. Generally speaking, as the temperature rises, the enhanced ion dissociation increases the concentration of charge carriers, further boosting ion conductivity and enhancing conductivity. The relationship between ion conductivity and surrounding temperature can be characterized using the Vogel-Tamman-Fulcher (VTF) equation[121]:

$$\sigma(T) = \sigma_{\infty} e^{-\frac{B}{(T-T_V)}}$$

where $\sigma(T)$ represents the ion conductivity; σ_{∞}, B, and T_V are material constants determined by the material.

Ge *et al.* proposed a strain-temperature dual-sensing hydrogel sensor inspired by the fiber structure of human muscles[122] [Figure 8A]. Polyaniline (PANI) NFs interwoven in the hydrogel enhance the self-healing ability and form strong hydrogen bonds and a "dynamic zipper" effect. The addition of glycerol inhibits water crystallization, improves freeze protection, and further promotes the sensor's sub-zero temperature self-healing, water retention, and adhesion properties. Thanks to the high thermal sensitivity of PANI NFs, the sensors exhibit excellent temperature coefficient of resistance (TCR) and temperature resolution (2.7 °C).

Wang *et al.* prepared an IL/TPU ionogel fibrous sensor consisting of TPU and IL using wet spinning techniques[123] [Figure 8B]. In addition to the excellent strain sensing properties, it can be made into a strain-sensitive temperature sensor with an S-shape. The temperature sensing error is within 0.15 °C when the sensor is simultaneously subjected to 30% tensile strain. Thanks to the fast and stable thermal response of IL, the temperature sensors show a monotonic temperature response over a wide temperature range (-15 to 100 °C) with a detection accuracy of 0.1 °C.

Humidity sensing capability

Information such as ambient humidity and sweat content on the skin surface is obviously important. Humidity sensing capabilities have significant application potential in biomedical, environmental monitoring and smart home scenarios[124-127]. A humidity sensor is a device that can detect the moisture content of the environment or the surface of an object and generate a characteristic electrical signal. According to the sensing mechanism, humidity sensors can be categorized as: resistive, piezoelectric, capacitive, optical, and semiconductive[128-131].

Humidity sensors using semiconductor heterojunctions can exhibit sensitive humidity sensing capabilities. Hou *et al.* prepared one using borophene-MoS_2 heterostructures, which has ultra-high sensitivity [up to 15,500% at a relative humidity (RH) of 97%][132], fast response, long lifespan, and good flexibility. In their recent work, the high-performance humidity sensor using a Borophene-BC_2N quantum dot heterostructures exhibits stronger performance[133], with an ultra-high sensitivity (up to 22,001% at 97% RH), wide detection range (11%-97%), low hysteresis, and extremely excellent stability. The advantage is best highlighted by the fact that the boronene-BC_2N heterostructure is 100 or 20 times more sensitive at 97% RH at room temperature compared to boronene (α′-4H-borophene) or BC_2N quantum dots alone. This sensor has strong potential for applications in flexible wearable and smart homes. It can be applied to diaper monitoring for infants and critically ill patients, wireless monitoring of respiratory behavior and speech recognition by detecting humidity in exhaled breath, and contactless switching by detecting humidity values on the surface of fingertips [Figure 9A].

Resistive humidity sensors are the most common of these and typically consist of a conductive element and a hydrophilic element [e.g., WS_2, polyimide (PI), polyvinyl alcohol (PVA), citric acid (CA), and hydroxyl ethyl cellulose (HEC)][134-137]. When moisture is absorbed by the sensor, it causes a change in the conductive path of the conductive element, resulting in an alteration in resistance or current[138]. Xu *et al.* prepared a carboxylated styrene-butadiene rubber (XSBR)/CA/silver nanoparticles (AgNPs) conductive film, where the Ag NPs formed conductive pathways by *in situ* diffusion in the XSBR matrix[134]. Due to the hygroscopicity of CA, this conductive film is sensitive to various humidity levels [Figure 9B].

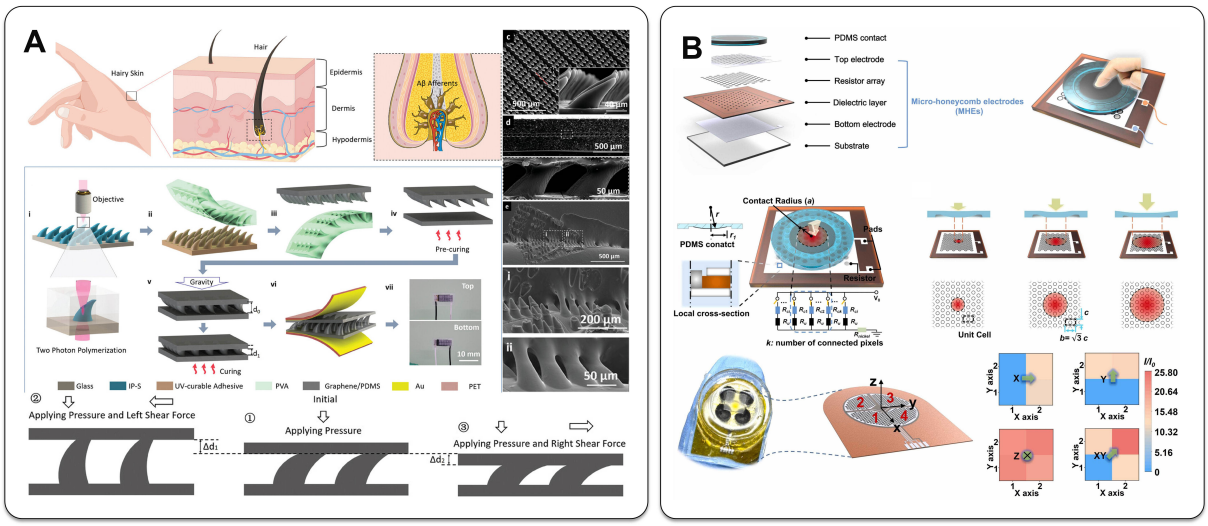

Figure 7. (A) The structure and sensing mechanism of shear force sensor with TMHAs[105]; (B) the design concept of multi-contact tactile sensors and mechanism of shear resolution[106]. UV: Ultraviolet; PVA: polyvinyl alcohol; PET: polyethylene terephthalate; PDMS: polydimethylsiloxane; TMHAs: tilted micro-hair arrays.

A clear trend is the preparation of more skin-conformable, breathable humidity sensors, which is manifested in nascent research by applying special strategies such as nanomesh[139,140], porous[141], fiber/textile[142], and paper matrices[143]. On the one hand, these strategies improve the comfort of wearing. On the other hand, they also increase the chance of contact between the sensor and the moisture to improve the sensor performance (high specific surface area)[144].

Li *et al.* proposed a humidity sensor (SAMP) based on poly(styrene-block-butadienstyrene) (SBS) NFs and alkalized MXenes/polydopamine (AMP) composites[135] [Figure 9C]. The SBS NFs provide an ultrathin, highly flexible and breathable substrate, and the skin-conformable, breathable, and sensing properties of this sensor have achieved significant progress due to its large specific surface area and abundant water-absorbing hydroxyl groups. The sensor has a Young's modulus (~0.10 MPa) similar to human skin (~0.13 MPa), high breathability (0.078 $g \cdot cm^{-2} \cdot d^{-1}$), high sensitivity (S = 704), and fast response/recovery (0.9 s/0.9 s).

Self-healing capability

Self-healing capability is an indispensable natural repair mechanism in the human life system, which is of vital significance to daily life, and enables the human body to recover from injuries, thus effectively safeguarding the health of the body. Similarly, it can greatly expand the lifespan and application scenarios of e-skins[145-148]. The basic strategy for this capability of e-skins is to fabricate e-skins using intrinsic self-healing polymers (SHPs)[149-151]. Such polymers are generally rich in reversible intermolecular interactions or dynamic covalent bonds within them and consist of two main types of materials: repairable plastics[152-155] and gels[156-158].

Liu *et al.* reinforced poly(vinylidene fluoride-co-hexafluoro propylene) (PVDF-HFP)/fluorosurfactant (FS3000) film with electro-spun PVDF-NFs to make PVDF-NFs/PVDF-HFP/FS3000 self-healing substrates[159]. This nanofiber-reinforced self-healing substrate has 836% and 1,000% higher tensile strength

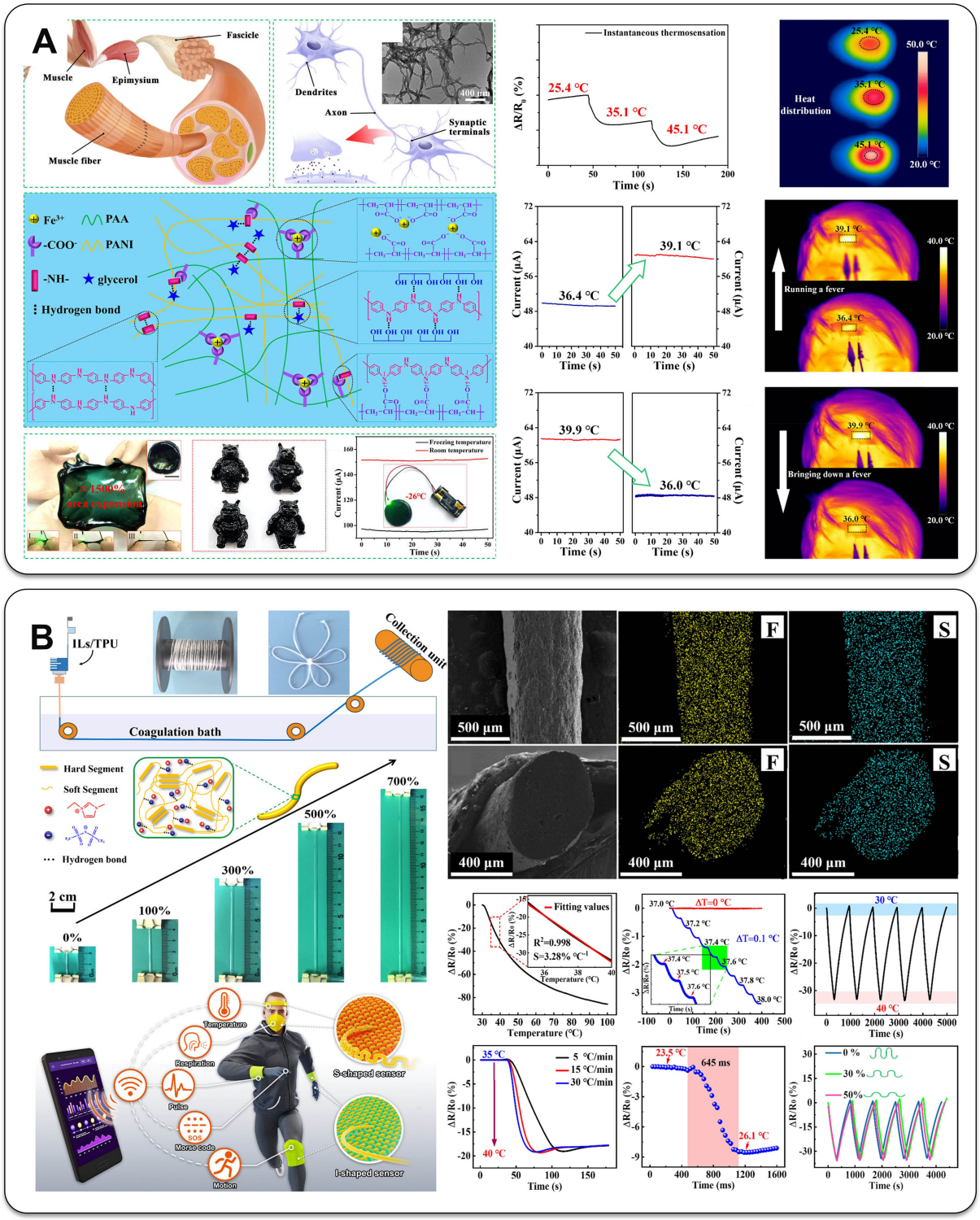

Figure 8. (A) The structure and temperature sensing properties of the muscle fiber-inspired strain-temperature dual sensing hydrogel sensor[122]; (B) the preparation method, structure and temperature sensing properties of the IL/TPU ionogel fibers[123]. PAA: Polyacrylic acid; PANI: polyaniline; ILs: ionic liquids; TPU: thermoplastic polyurethane.

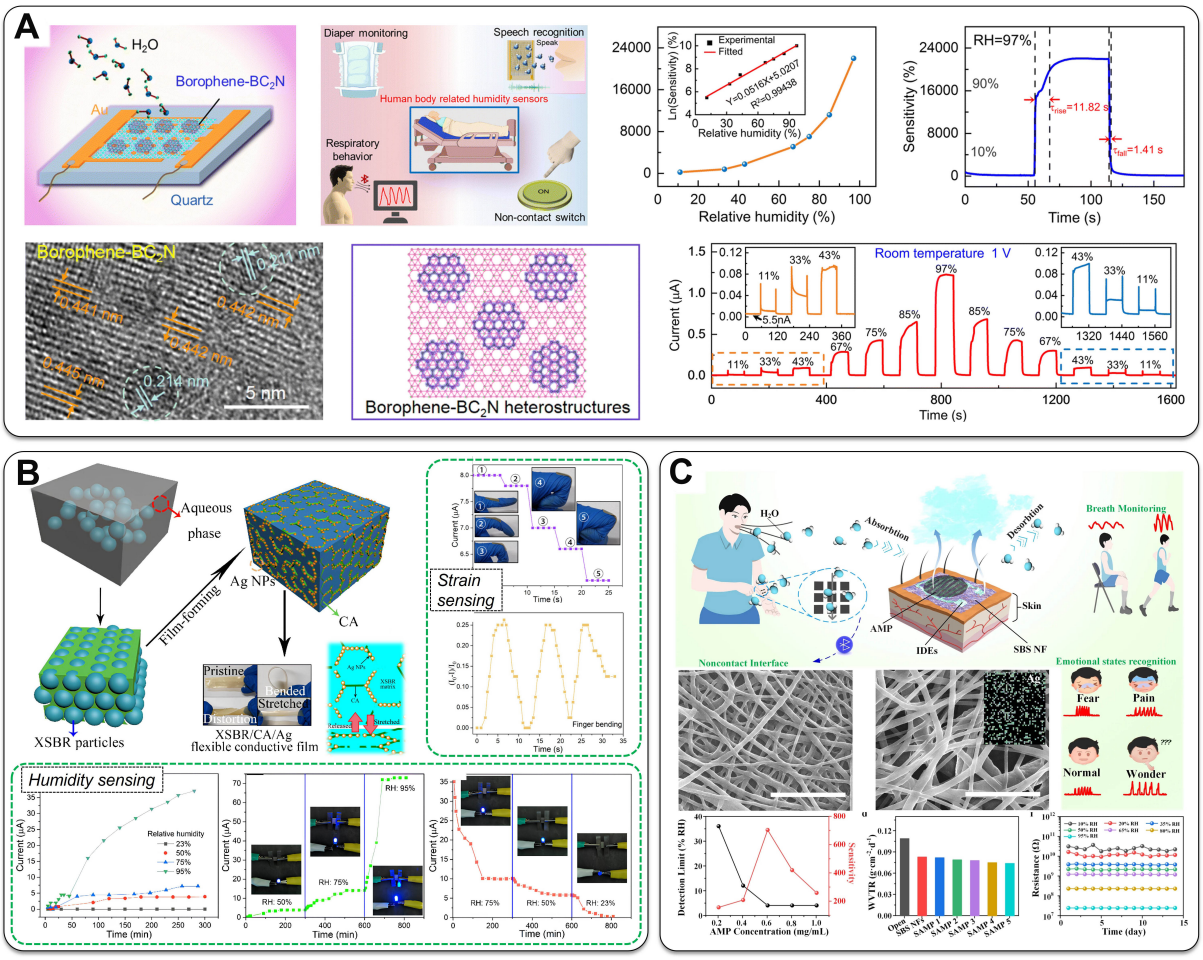

Figure 9. (A) heterostructures, flexible wearable application, and humidity sensing performance of Borophene-BC_2N quantum dot humidity sensor[133]; (B) the microstructure, strain sensing and humidity sensing properties of XSBR/CA/AgNPs conductive films[134]; (C) the microstructure, humidity sensing performance, and application scenarios of the SAMP sensor[135]. RH: Relative humidity; NPs: nanoparticles; CA: citric acid; XSBR: carboxylated styrene-butadiene rubber; AMP: alkalized MXenes/polydopamine; SBS: poly(styrene-block-butadienstyrene; NF: nanofiber.

and toughness, respectively, than the pure PVDF-HFP/FS3000 substrate, and also shows greatly improved healing efficiency, allowing self-healing within 24 h at room temperature. Subsequently, e-skin devices were fabricated with the self-healing substrate and two functional layers (detection and heating layers). What is more attractive is that they also designed a related program that collects signals from the detection layer and automatically sends commands to the heating layer when the device is damaged by external forces, accelerating the healing process through Joule heat, demonstrating a destruction-healing process that is closer to that of the human body [Figure 10A][159-161].

Gel materials, with a large number of hydrogen-bonded dynamic cross-links and supramolecular interactions within, possess a good self-healing ability, which, coupled with excellent biocompatibility, adhesion, and ductility, makes it an ideal candidate for self-repairing sensors[162-165].

Wei *et al.* prepared a Clay poly[2-(2-Methoxyethoxy) ethyl methacrylate-co-oligo(ethylene glycol) methacrylate] [Clay/P(MEO_2MA-co-OEGMA)] conductive gel with glycerol-water as a binary solvent by *in situ* gelation on the clay surface[160] [Figure 10B]. The prepared gels show high flexibility, extensibility

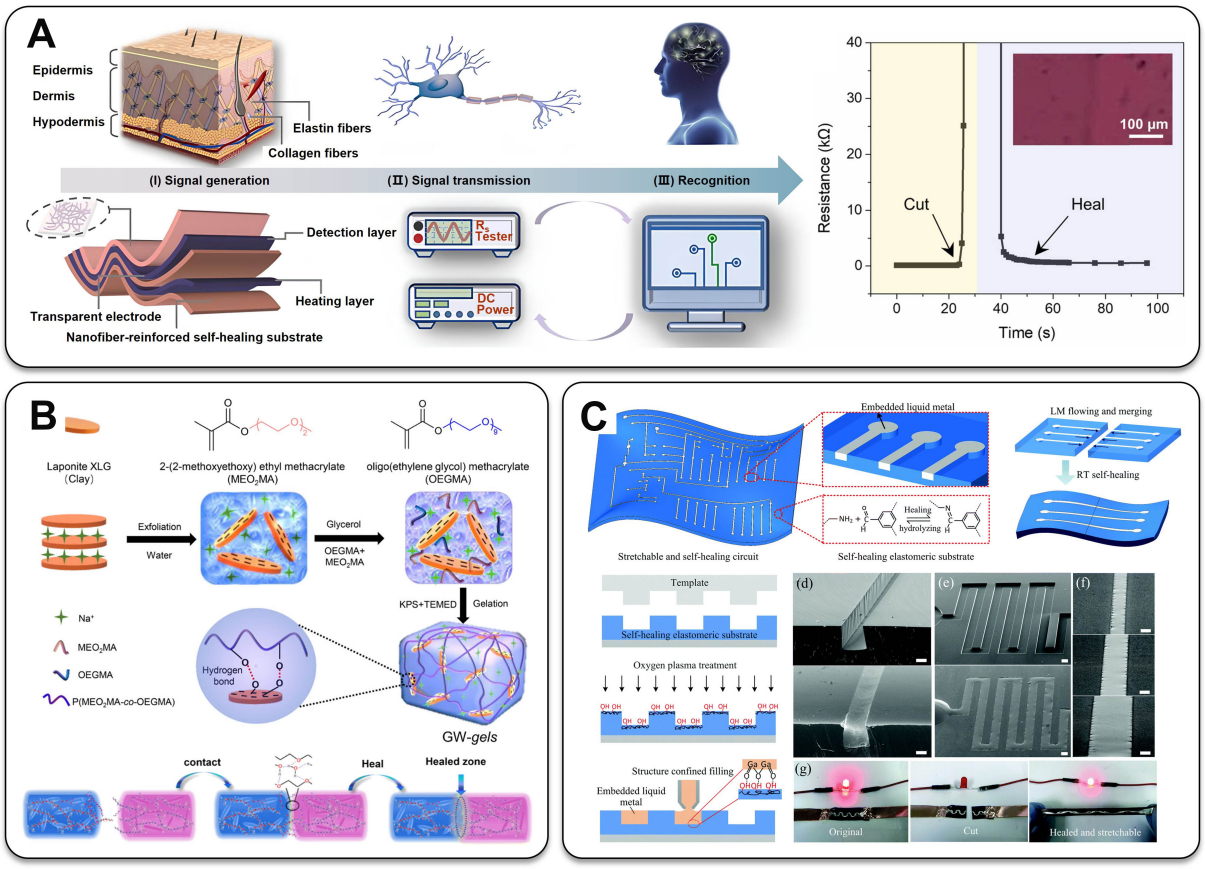

Figure 10. (A) the self-healing process and resistance change of the PVDF-NFs/PVDF-HFP/FS3000 e-skin[159]; (B) the structure and healing mechanism of the Clay/P(MEO_2MA-co-OEGMA) sensor[160]; (C) the structure of PDMS/MWCNT+LM capacitive strain sensing e-skin[161]. Laponite XLG Clay: 92.32 wt.% $[Mg_{5.34}Li_{0.66}Si_8O_{20}(OH)_4]Na_{0.66}$ and 7.68 wt.% $Na_4P_2O_7$; KPS: potassium persulfate; TEMED: N,N,N′,N′-tetramethylethylenediamine; GW: glycerol-water cosolvent; LM: liquid metals; RT: room temperature; PVDF: polyvinylidene fluoride; NFs: nanofibers; HFP: hexafluoro propylene; P(MEO_2MA-co-OEGMA): poly(methoxyethyl acrylate-co-oligo(ethylene glycol) methacrylate; PDMS: polydimethylsiloxane.

(elongation ~600%), and conductivity (~3.32 × 10^{-4} S·cm^{-1}), and the abundant hydrogen bonding interactions between the clays and the P(MEO_2MA-co-OEGMA) chains contribute to a good self-healing ability (healing efficiency of 84.8%).

On the other hand, the self-healing function of e-skins needs to repair not only mechanical damage but also damage to the conductive pathways inside the device[166-168]. A fashionable approach is to use liquid metals (LM) with high conductivity and fluidity, such as eutectic gallium indium (EGaIn) alloys, Fe-particle doped EGaIn (Fe-EGaIn), to make e-skins[169-174]. The LM will form a shell with the surrounding resin matrix and air, encasing it inside. When the device is damaged, this shell ruptures and the LM inside will flow out, re-forming the conduction path and a new shell, where the resin matrix obviously also serves as an encapsulation in the device[175-180].

Chen *et al.* fabricated a self-healing resin matrix + LM capacitive strain sensing e-skin by combining nanoimprinting and printing technologies [Figure 10C] MWCNT-reinforced reversible imine-bonded self-healing poly (dimethylsiloxane) elastomers (PDMS/MWCNT) were used as the substrate, and their good imprintability was utilized to prepare embedded LM patterned circuits, which were assembled to form a capacitive strain sensor that is fully stretchable and self-healing[161]. The related e-skin possesses extremely

strong self-healing properties, with a healing efficiency of 94.3% in 1 h for the PDMS/MWCNT matrix alone.

Shi *et al.* report a heterogeneously integrated e-skin system of dynamically covalently bonded polyimide (encapsulation and matrix) + liquid eutectic LM (electrical and sensing) + chip (information processing), which simultaneously provides full recyclability, excellent mechanical stretchability, self-healing and reconfigurability[181]. The polyimide matrix with an active bond exchange reaction network and the fluidity of LM enable this e-skin system to self-heal from damage and re-adapt to the current application scenario. All materials and components involved are recyclable.

Brief summary

This section summarizes the six most common basic capabilities of e-skins: pressure, strain, shear, temperature, humidity, and self-healing.

Overall, resistive sensing mechanisms are the most used, thanks to their easy and reliable detection and the rich possibilities in device architecture design. In addition, e-skins employing triboelectric and piezoelectricity can be developed into self-powered e-skins, which can be used in the future as power supply units in integration with other e-skins.

From the material point of view, e-skins can be classified into two main categories: FCPCs and conductive gels. FCPCs are classified into polymer matrix and conductive materials. For the former, flexible polymer materials, such as PDMS, TPU, SBS, cellulose, paper, *etc*., are widely used[182], in which PDMS is popular for its excellent flexibility, transparency, and process adaptability. Commonly used conductive materials include one-dimensional materials, such as silver nanowires (AgNWs), copper nanowires (CuNWs), and CNTs, two-dimensional materials, such as reduced GO (rGO) and MXene[183], and highly conductive materials such as Ag NPs, LM, and carbon black (CB).

E-skins constructed using conductive gel materials have a higher sensing range but tend to exhibit larger response time, and lower durability, which comes from their traditional characteristics such as low modulus and low toughness. However, they tend to be irreplaceable in terms of biocompatibility and adhesion, and scientists have also been trying to improve their performance and shortcomings. Their performance has been greatly improved in recent years. A typical example is the "Salting Out-Alignment-Locking" design recently adopted by Sun *et al.* to greatly improve the tensile strength, modulus and toughness of gelatin hydrogels. The tensile strength, modulus, and toughness of gelatin hydrogels can be increased up to 940, 2,830, and 1,785 times, respectively[184].

The structure, material, mechanism and main characteristic parameters of some classic e-skins have been listed in Table 1.

COMPLEX E-SKIN SYSTEMS

In fact, the perception of human skin of external stimuli is seldom a single sense or sensing unit acting alone. Typically, for example, when a drop of water is dropped on our skin, most of the time, it is perceived through a combination of temperature and humidity sensing, plus pressure sensing if the drop is heavy enough and falling fast. On the other hand, all responses and processing of stimulus signals require the intervention of information processing units such as the nervous system so that more advanced human-environment interactions can be achieved (for e-skins, it is HMI). Therefore, single-sensing systems are insufficient, and the scientists have been conducting research on complex e-skin systems such as multimodal, IoT-integrated, and ML-enabled e-skin systems.

Table 1. Structure, material, mechanism and main characteristic parameters of some classic e-skins

Sensing type	Material	Structure	Sensing mechanism	Sensitivity	Sensing range	Respond time [trigger/release]	Durability	Ref.
Pressure*	PANI coated rGO on textile substrate	Filled-type FCPCs	Resistive	Sp = 97.28 kPa^{-1}	0.0005~40 kPa	30/25 ms	11,000	[40]
Pressure	CB/TPU	Porous filled-type FCPCs	Resistive	Sp = 1.55 MPa^{-1}	Max = 584.4 kPa	150/150 ms	10,000	[42]
Pressure	CNT-PGS foam	Porous filled-type FCPCs	Resistive	Sp = 8.00 ± 0.20 kPa^{-1}	0.1~8 kPa	≤ 20 ms	220,000	[45]
Pressure*	CNTs/PDMS	Interlocked microdome array	Resistive	Sp = 2.21 N^{-1}	0.1~20 kPa	-	-	[46]
Pressure	CNTs/PDMS	Interlocked microdome array	Resistive	Sp = -15.1 kPa^{-1}	0.0002~59 kPa	~ 40 ms	-	[47]
Pressure	PEDOT on a 3D-printed substrate	Interlocked microdome array + nano contacts	Resistive	Sp = 184.82 kPa^{-1} (< 10 kPa)	0.06~39.2 kPa	0.038/0.045 ms	1,000	[48]
Pressure	ZnO nanowires array on PDMS substrate	Interlocked microdome array + nano contacts	Resistive	Sp = -6.8 kPa^{-1}	Min = 0.0006 kPa	< 5 ms	1,000	[49]
Pressure*	Wrinkle CNTs (humidity sensing part)/PDMS on a porous CNT/PDMS substrate (pressure sensing part)	Porous	Resistive	Sp = 0.537 kPa^{-1} (< 3 kPa), 0.007 kPa^{-1} (> 3 kPa)	-	78/62.5 ms	10,000	[50]
Pressure*	CNTs/PDMS-Ni electrodes/resistor array/PI dielectric/Ni electrodes	Resistor array + Micro-honeycomb electrodes	Resistive	Sp = 25.88 kPa^{-1} (large range mode), 64.68 kPa^{-1} (high sensitivity mode)	Max = 1,400 kPa (large range mode), 500 kPa (high sensitivity mode)	133/73 ms	2,000	[106]
Pressure	SBS/AgNP coated-kevlar fiber textiles	Capacitive fiber textiles	Capacitive	Sp = 0.21 kPa^{-1}	Max = 3.9 MPa	< 10 ms	10,000	[54]
Pressure	Ag pyramid array (top electrode)/ATMP-PVA hydrogel film (dielectric layer)/Ag (bottom electrode)	Pyramid array electrode + dielectric layer	Capacitive	Sp = 3,224.2 kPa^{-1}	Max = 100 kPa	~6 ms	200	[56]
Pressure	PI/interlocked P(VDF-TrFE)/Cu	Interlocked pyramid array	Capacitive	Sp = 6.583 kPa^{-1}	Min = 3 Pa	48/36 ms	10,000	[60]
Pressure*	TPU/MXene/AgNWs-TPU-TPU/MXene/AgNWs	Two filled-type FCPCs sandwiched a dielectric layer	Capacitive	Sp = 0.029 kPa^{-1}	0~70 kPa	260/- ms	2,000	[73]
Pressure*	Carbon fabric + CIP/PDMS flagella array + carbon fabric	Parallel plate + unilateral flagella array	Capacitive	Sp = 0.0124 kPa^{-1}	0.002~100 kPa	~100/100 ms	~2,000	[103]
Pressure*	rGO/PDMS	Parallel plate + unilateral tilted microhair array	Capacitive	Sp = 0.0513 kPa^{-1} (0.03 < 6 kPa), 0.0079 kPa^{-1} (6~120 kPa), 0.0009 kPa^{-1} (120~300 kPa)	0.03~300 kPa	60/54 ms	5,000	[105]
Pressure	PDMS/PTFE/AgNWs/PDMS TENG	Interlocked conical array	Triboelectric	Sp = 127.22 mV·kPa^{-1}	5~50 kPa	-	5,000	[61]
Pressure	Nylon/PDMS pyramid array/TPU/AgNWs TENG	Pyramid array	Triboelectric	Sp = 9.973 mV·Pa^{-1} (0-1.6 kPa), 0.538 mV·Pa^{-1} (> 1.6 kPa)	Max > 6 kPa	-	1,000	[66]

Pressure	GO-PVDF/BTO Piezoelectric NFs textiles + PU substrate	Piezoelectric fiber textiles	Piezoelectric	Sp = 10.89 ± 0.5 mV·kPa^{-1}	80~230 kPa	-	8,500	[62]
Strain*	PANI coated rGO on textile substrate	Filled-type FCPCs	Resistive	GF = -78	Max = 10%	-	1,000	[40]
Strain*	CNTs/PDMS	Interlocked microdome array	Resistive	GF = 27.8 (0%-40%), 1,084 (40%-90%), 9,617 (90%-120%)	Max = 120%	18/10 ms	-	[46]
Strain	AgNW/DS on strain-engineered stretchable substrate	Patterned circuit	Resistive	GF = ~4.5 (0%~25%), ~33 (25%~68%)	0%~68%	-	1,000	[80]
Strain	Pre-stretching CNTs@TPU fiber felt	Micro-cracks + micro-contacts	Resistive	GF = 428.5 (0%~100%), 9,268.8 (100%~220%), 83,982.8 (220%~300%)	0%~300%	70/70 ms	10,000	[81]
Strain	Vertical graphene on PDMS	Micro-cracks	Resistive	GF > 5,000	0%~30%	200/100 ms	10,000	[82]
Strain	Laser scribed graphene	Micro-cracks	Resistive	GF = 11 (0%~2.5%), 92 (2.5%~4.5%), 673 (4.5%~5%)	0%~10%	-	1,000	[83]
Strain	PDMS/GO/PDMS	Sandwich-type FCPCs + micro-cracks	Resistive	GF = 2,175.8	-	-	1,000	[84]
Strain	NR-NR/CNT-NR	Sandwich-type FCPCs + micro-cracks	Resistive	GF = 2,280	Max = 500%	21 ms	2,000	[85]
Strain	PDMS/GO/PDMS	Sandwich-type FCPCs + micro-cracks	Resistive	GF = 1,054	Max = 26%	-	500	[87]
Strain	Ti_3C_2Tx MXene/CSPMXPy-x/Fe^{3+}+Cu^{2+} hydrogels	Mxene filled-hydrogels	Resistive	GF = 4.64	Max > 300%	-	100	[90]
Strain	SN-PAAM hydrogels	Conductive hydrogels	Resistive	GF = 1.62~2.46	Max = 1,836%	120~130 ms	200	[91]
Strain	PVA/NaCl hydrogels	Conductive hydrogels	Resistive	GF < 2.1	0.5%~100%	-	200	[93]
Strain	PU-IL ionogels	Conductive ionogels	Resistive	GF = 1.54	0.1%~300%	-	1,000	[100]
Strain*	PPBN-hydrogel	Conductive hydrogels	Resistive	GF = 18.28	6%~268.9%	-	1,000	[122]
Strain*	ILs/TPU ionogel fiber	Conductive ionogel fiber	Resistive	GF = 3.35	0.05%~700%	170/120 ms	2,000	[123]
Strain*	TPU/MXene/AgNWs-TPU-TPU/MXene/AgNWs	Two filled-type FCPCs sandwiched a dielectric layer	Capacitive	GF = 1.21	0%~150%	210/280 ms	2,000	[73]
Shear*	CNTs/PDMS-Ni electrodes/resistor array/PI dielectric/Ni electrodes	Pressure sensor array	Resistive	Ss = 36.137 N^{-1}	0-1.5 N	-	-	[106]
Shear*	Carbon fabric + CIP/PDMS flagella array + carbon fabric	Parallel plate + unilateral flagella array	Capacitive	Ss = 0.0752 N^{-1} (0.015~0.50 N), 0.0177 N^{-1} (0.50-1.30 N)	0.015~1.3 N	-	-	[103]

Shear*	rGO/PDMS	Parallel plate + unilateral tilted microhair array	Capacitive	Ss = -0.0134 kPa^{-1} (left), 0.0195 kPa^{-1} (right)	1.5~30 kPa (left) 0.3~6 kPa (right)	-	1,000	[105]
Temperature	PEDOT@TPU fiber	Core-shell fiber	Resistive	TCR = 0.95% $°C^{-1}$	20~40 °C	30/27 s	-	[117]
Temperature*	PPBN-hydrogel	Conductive hydrogels	Resistive	TCR = 1.64% $°C^{-1}$	40~110 °C	-	-	[122]
Temperature*	ILs/TPU ionogel fiber	Conductive ionogel fiber	Resistive	TCR = 3.28% $°C^{-1}$	-15~100 °C	645/- ms	-	[123]
Humidity*	Wrinkle CNTs (humidity sensing part)/PDMS on a porous CNT/PDMS substrate (pressure sensing part)	Wrinkle surface	Resistive	S_h = 0.0055/RH % (15%-60% RH), 0.0323/RH % (60%-85% RH)	Max = 85% RH	-	-	[50]
Humidity	AgNWs/etched Al foil/SiO_2 moisture sensitive layer/Cu	Multilayer fabric and porous structure	Resistive	S_h = 0.3007/RH % (10%~70% RH), 13.1667/RH % (70%~92% RH)	10%~92% RH	25/55 s	3	[126]
Humidity	SBS nanofibers/AMP	Moisture sensitive fiber felt	Resistive	R = 704	10%~95% RH	0.9/0.9 s	5	[138]
Humidity	WCN	Moisture sensitive capacitor bridge	Capacitive	S_h = 4.479 (20%~94% RH) R = 2,152	7%-94% RH	20/6 s	-	[129]
Humidity	Borophene-MoS_2	Borophene-MoS_2 heterostructures	Semiconductive	S_h (%) = 15,500%	0%~97% RH	2.5/3.1 s		[132]
Humidity	Borophene/BC_2N QD	Borophene-BC_2N QD heterostructure	Semiconductive	S_h (%) = 22,001%	11%~97% RH	11.82/1.41 s	-	[133]

*means it is a multimodal e-skin. Definition of sensitivity parameters: Pressure sensor --- $Sp = \delta(\Delta J/J0)/\delta P$, sensitivity, where $\Delta J/J0$ is the relative change of the concerned parameter (resistance, current, capacitance, voltage, *etc.*), and P is the applied pressure; Strain sensor --- $GF = \delta(\Delta J/J0)/\delta\varepsilon$, gauge factor, where $\Delta J/J0$ is the relative change of the concerned parameter (resistance, current, capacitance, *etc.*), and ε is the applied strain; Shear force sensor --- $Ss = \delta(\Delta J/J0)/\delta F$, sensitivity, where $\Delta J/J0$ is the relative change of the concerned parameter (resistance, current, capacitance, *etc.*), and F is the applied shear force; Temperature sensor --- $TCR = \delta(\Delta J/J0)/\delta T$, temperature coefficient of resistance, where $\Delta J/J0$ is the relative change of resistance, T is the temperature; Humidity sensor --- $Sh = \delta(\Delta J/J0)/\delta RH$, sensitivity, where $\Delta J/J0$ is the relative change of the concerned parameter (resistance, current, capacitance, voltage, *etc.*), and RH is the relative humidity; $Sh\ (\%) = (I - I0)/I0 \times 100\%$, sensitivity of humidity, where I and $I0$ represent the current in a given RH and dry air, respectively; $R = Jc/J0$, response amplitude, where Jc and $J0$ are the concerned parameters at a certain and a fixed RH. PANI: Polyaniline; rGO: reduced graphene oxide; FCPCs: flexible conductive polymer composites; CB: carbon black; TPU: thermoplastic polyurethane; PGS: poly(glycerol sebacate); CNTs: multiwall carbon nanotubes; PDMS: polydimethylsiloxane; PEDOT: poly(3,4-ethylenedioxythiophene); SBS: poly(styrene-block-butadienstyrene); AgNP: silver nanoparticle; ATMP-PVA: polyvinyl alcohol; P(VDF-TrFE): poly(vinylidenefluoride-co-trifluoroethylene); AgNWs: silver nanowires; CIP: carbonyl iron particles; PTFE: polytetrafluoroethylene; TENG: triboelectric nanogenerator; PU: polyurethane; GO-PVDF: graphene oxide-polyvinylidene fluoride; BTO: barium titanate; NFs: nanofibers; GF: gauge factor; DS: Dragon Skin 30; NR: natural rubber; SN-PAAM: sodium dodecyl sulfate-modified poly(acrylamide) hydrogel; PVA: polyvinyl alcohol; IL: ionic liquid; ILs: ionic liquids; PI: polyimide; CIP: carbonyl iron particles; RH: relative humidity; AMP: alkalized MXenes/polydopamine; WCN: wood-derived cellulose nanopaper; QD: quantum dot.

Multimodal e-skin systems

Integration of multiple sensing capabilities (multimodal e-skins) is necessary to achieve a high level of sensing capability[37,185,186]. Scholars have fabricated excellent multimodal e-skin systems through exquisite material and structural design[187-190].

Some scholars prepare multimodal e-skins with multifunctional materials, which embody two or more sensing properties[191]. However, it is difficult for such multimodal e-skins to achieve excellent comprehensive performance, and it is difficult to avoid interference between various sensing characteristics. Various sensing characteristics often cannot reflect outstanding performance at the same time.

In contrast, integrating multiple types of sensing devices with superior performance into the same e-skin device can achieve better overall performance. In such multimodal e-skins, dealing with the interference problem between different sensing characteristics remains an important issue[192], which is a major shackle restricting the performance of the multimodal e-skin system[112,117,123,193].

A common solution is to independently integrate multiple sensors into a single e-skin device, with each sensor having its own dedicated independent signal transmission line[194]. As shown in [Figure 11A], Zhao *et al.* reported a flexible pressure-strain multimodal sensor capable of sensing both signals of external force magnitude and direction simultaneously[195]. Three-dimensional tubular graphene sponge (3D-TGS) and spider web-like electrodes were used as pressure-sensitive and strain-sensitive modules, respectively. By comparing the output signals, the magnitude and direction of the force can be monitored simultaneously.

Hua *et al.* prepared a highly stretchable conformal matrix network (SCMN) on a polyimide network [Figure 11B], which can be fabricated into a multisensory e-skin able to simultaneously sense multiple stimulus signals through the selection of different sensing components, including temperature (Pt-sensitive layer), humidity (Al/PI-sensitive layer), plane strain (Constantan-sensitive layer), ultraviolet (UV, Al/ZnO-sensitive layer), magnetism (Co/Cu multilayer-sensitive layer), pressure, and proximity, thereby realizing multimodal sensing with a tunable range of sensing and large scalable area[196].

Such structures can avoid interference problems, but they also bring about the problem of complex structure, which is disadvantageous in the development trend of high density and miniaturization. Some scholars avoid this interference by carefully designing the structure of the e-skin systems. Lin *et al.* reported a piezoelectric tactile sensor array with both pressure sensing and bending sensing capabilities[197] [Figure 11C]. The specially designed insulating layer and structural design of the row + column electrodes can greatly alleviate the crosstalk problem in other sensors. A signal processor and logic algorithms were also integrated to enable real-time sensing and differentiation of the magnitude, location, and pattern of various external stimuli, including gentle sliding, touching, and bending. Pressure sensing and bending sensing tests show that the proposed haptic sensor array has high sensitivity (7.7 $mV \cdot kPa^{-1}$), long-term durability (80,000 cycles), and faster response time (10 ms) than human skin.

IoT-integrated and ML-enabled e-skin systems

In recent years, the integration of e-skins in the IoT has become a clear trend, as it allows for the rationalization of e-skins with other cutting-edge technologies, such as advanced mechanics and ML methods, to create intelligent systems, which is the key to allowing e-skin to be truly integrated into human-machine systems. Advances in this field are expected to open up entirely new applications in areas such as health monitoring, wearable electronics, and robotics[198].

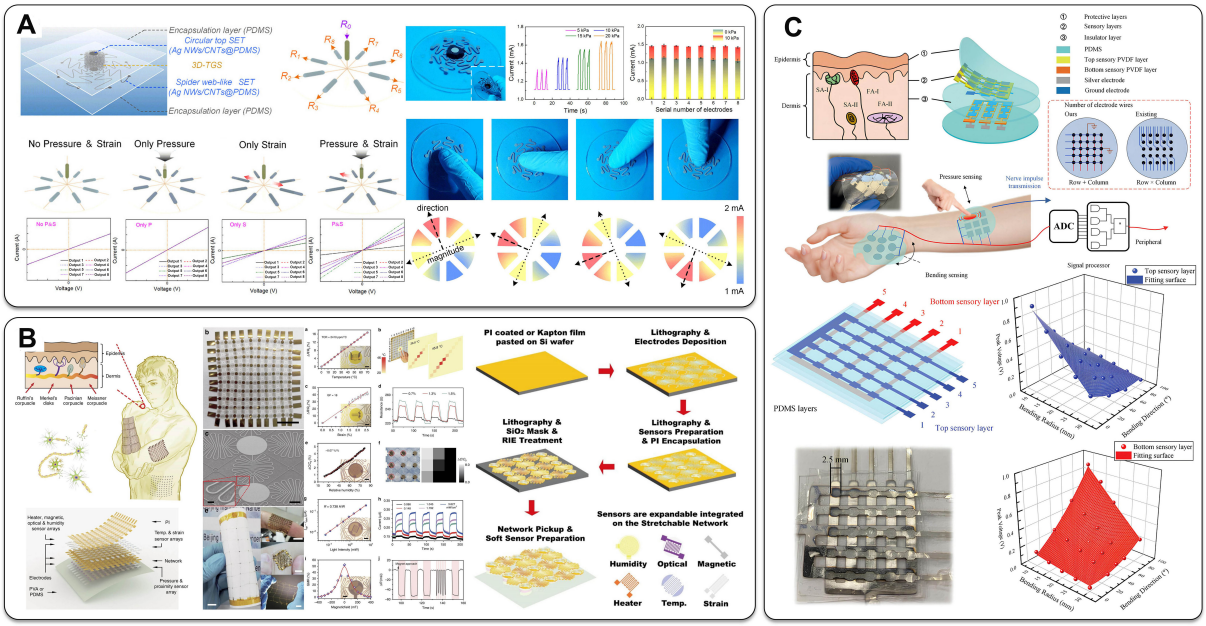

Figure 11. (A) The multimodal sensing characterization and mechanism of the spider web-like flexible tactile sensor[195]; (B) the structure, multimodal sensing properties (temperature, humidity, plane strain, ultraviolet, magnetism, *etc.*), and preparation process of a highly flexible and stretchable matrix network e-skin[196]; (C) composition of the skin-inspired piezoelectric tactile sensor array system and comparison with human skin[197]. PDMS: Polydimethylsiloxane; SET: stretchable electrode; PI: polyimide; PVA: polyvinyl alcohol; PVDF: polyvinylidene fluoride; ADC: analogue-to-digital converter.

The basic strategy is to use hardware devices with information processing capabilities, such as Micro-Controller Unit (MCU), Digital Signal Processor (DSP), Field-Programmable Gate Array (FPGA), *etc.*, as the control center to receive sensing signals and process them through specific program burned before. In this way, e-skins can be combined with other components (such as actuators, power supplies, and other e-skins) to form a powerful and intelligent IoT system.

Zhang *et al.* developed carboxyethyl chitin/polyacrylamide (CECT/PAM) hydrogels with high transparency (92%), high conductivity (0.62 $S \cdot m^{-1}$), ultra-flexibility (strain up to 1,586%, toughness up to 1,300 $kJ \cdot m^{-3}$), good fatigue resistance, and strong adhesion ability and used them to make wearable devices including RSSs, capacitive pressure sensors, and TENGs with good performance[199]. Sign language recognition and spatial perception of pressure were achieved using an STC89C52 MCU to process data from the hydrogel-based strain sensor and pressure sensor array [Figure 12A][199,200].

Chen *et al.* successfully simulated the force sensing system of human body by combining an In-doped ZnO memristors artificial synaptic device with Pt/CNFs strain sensors for stimulus detection and information processing using an Arduino Leonardo (ATmega32U4 chip) MCU[13] [Figure 12B]. The Pt/CNFs strain sensors applied the microcracking principle, where microcracks formed during stretching are bridged by the carbon NFs (CNFs), allowing the sensor to finely detect human motion and convert mechanical stimuli into electrical signals. The In-doped ZnO memristors synaptic device can mimic various basic properties of neuronal synapses and further process the information from the Pt/CNFs strain sensors based on the Spike-Rate-Dependent Plasticity (SRDP) behavior (which is actually a form of ML at the hardware level) after the MCU has converted the sensor signals into a sequence of pulses with different frequencies. By installing five strain sensors on the finger joints, it is demonstrated that the system can recognize gestures with high accuracy.

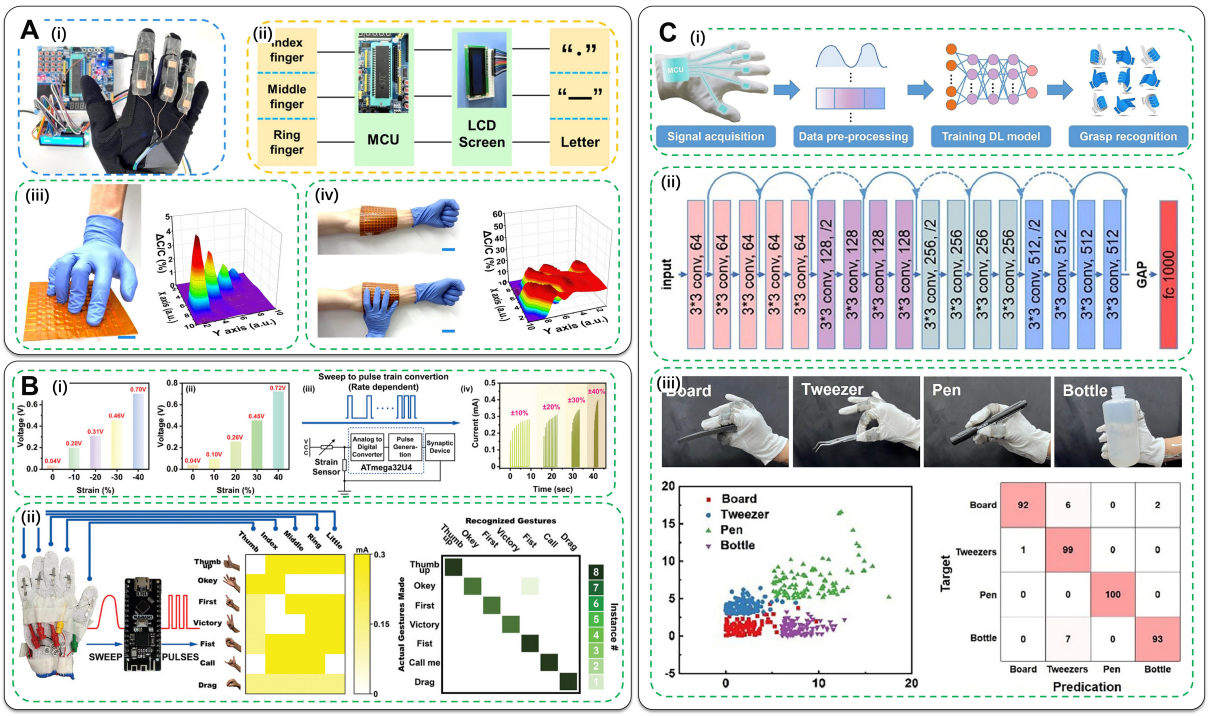

Figure 12. (A) Schematic diagram of (i) composition of the monolithcic integrated sensing system based on CECT/PAM hydrogels, (ii) the signal processing circuit, (iii) array of pressure sensors under four-finger contact and the corresponding signaling diagram, (iv) wearability of the e-skin system and the signaling diagram[199]; (B) Schematic diagram of (i) process from sensing to signal processing, (ii) gesture recognition system and its recognition results[13]; (C) Schematic diagram of (i) composition of NWF/AgNWs-MXene/PBSE multi-sensor system, (ii) structure of ResNet18 signal classification neural network, and (iii) various grasping actions and their classification results[200]. MCU: Micro-Controller Unit; CECT: carboxyethyl chitin; PAM: polyacrylamide; NWF: nonwoven fabrics; AgNWs: silver nanowires; PBSE: polyborosiloxane elastomer.

ML methods can greatly enhance the intelligence level of an e-skin system, which can greatly improve the performance of human-machine interfaces (HMI), and show a broad application prospect in medical health, rehabilitation therapy and remote monitoring[201-204]. They can learn feature signals corresponding to a certain stimulus from a large amount of experimental data, which can recognize different types of stimuli (such as gesture, touch strength, texture, and shape)[205-208].

ML models need to be trained on collected data before they can be put into use, and a signal collection system is necessary[209]. Therefore, ML-enabled e-skin systems are often further developed based on IoT-integrated e-skin systems.

Wang *et al.* constructed a wireless sensing grasping action recognition system using an MCU to collect signals from a prepared nonwoven fabrics (NWF)/AgNWs-MXene/polyborosiloxane elastomer (PBSE) multi-sensor system and combined it with a deep learning method to achieve accurate grasping action recognition[200] [Figure 12C].

Wang *et al.* built an artificial neural network (ANN) with a fully-connected structure to learn the data from a large number of tiny tactile sensors on the prepared tactile sensing gloves and realized the recognition of objects with different hardnesses and shapes, grasping motions for four kinds of fruits (with the highest recognition accuracy up to 99.26%), and grasping motions for seven kinds of objects ranging from soft to hard (with the highest recognition accuracy up to 99.35%)[210].

Niu *et al.* built an intelligent material sensing system by building a multilayer perceptron (MLP) neural network and making it learn the collected capacitive response data of the all-fabric bionic (AFB) e-skin to different materials in proximity and pressure modes[211]. The system can accurately discriminate nine materials with fuzzy morphology and smooth surfaces by the differences in dielectric constants and hardness of the materials, with an average accuracy of 96.6%.

Kim *et al.* presented a novel e-skin system integrated with a deep neural network[212]. It has a fine laser-induced crack structure to detect small deformations, captures dynamic motion without creating a sensor network, and, in combination with a deep neural network, a single skin sensor can discriminate the motion of the corresponding body part.

Tan *et al.* built a bioinspired spiking multisensory neural network (MSeNN) that integrates vision, touch, hearing, simulated smell and taste with cross-modal learning via ANNs[213]. Through distributed multi-sensors and bionic layered architecture design, it not only senses, processes, and memorizes multimodal data but also fuses multisensory data at both hardware and software levels.

APPLICATIONS OF E-SKINS

Scholars have been working hard to expand the application areas of e-skins. Here, we will briefly introduce the applications of e-skins, which can be simply divided into two major application fields: (1) wearable electronics and healthcare and (2) intelligent machinery. The former is the field of most concern. It is worth mentioning that there are not very clear boundaries between different applications.

Wearable electronics and healthcare

E-skins are invented to mimic human skin, making them naturally suitable for use in the healthcare and wearable fields[36]. The application environments often require the corresponding e-skin devices to possess various qualities such as non-toxicity, harmlessness, high flexibility, strong biocompatibility, chemical stability, comfort, high adhesion, and reconfigurability. Materials such as gels, soft metals (mainly precious metals with high chemical stability in physiological environments, such as Ag and Pt), PDMS, PI, and cellulose are widely used[5]. Typical application scenarios include detection and recognition of human limb movements, continuous monitoring of signals such as electrocardiogram (ECG), electromyogram (EMG), electroencephalogram (EEG), *etc.*, and detection of human body fluids (sweat, water vapor, excretory fluids, *etc.*)[214].

As shown in [Figure 13A], Gao *et al.* fabricated a composite hydrogel [poly(vinyl alcohol)/microfiber composite hydrogel (PVA/MF-CH) and PVA/MF/Glycerol-CH (PVA/MF/Gly-CH)] composed of PVA hydrogel and PU microfiber network embedded using electrospinning and spin-coating[215]. In addition to the common excellent ionic conductivity, freezing resistance, and dehydration resistance, their thickness (< 5 μm), Young's modulus (~0.04 MPa), and tensile strength (~6 MPa) are adjustable, so they possess better mechanical compatibility with human organs and tissues, which is of great significance in complex application environments, such as wearable and implantable bioelectronic devices, and are suitable for healthcare applications. Finally, the flexible electrodes prepared with them demonstrated their potential for long-term monitoring of electromyographic (EMG) bio-signals. Sun *et al.* proposed a green and sustainable one-pot synthesis method by *in situ* photopolymerization of polymerizable deep eutectic solvents (PDES) - treated cellulose pulp, and the prepared cellulose-based Ion conductors (ICs), PDES/cellulose microfibers (CMFs), exhibited very high stretchability (3,210% ± 302%), high ionic conductivity (0.09 $S \cdot m^{-1}$), high toughness (13.17 ± 2.32 $MJ \cdot m^{-3}$), strong self-healing ability, good stability, and compatibility with human skin[216]. The detection of typical human strain signals and ECG signals using flexible electrodes prepared

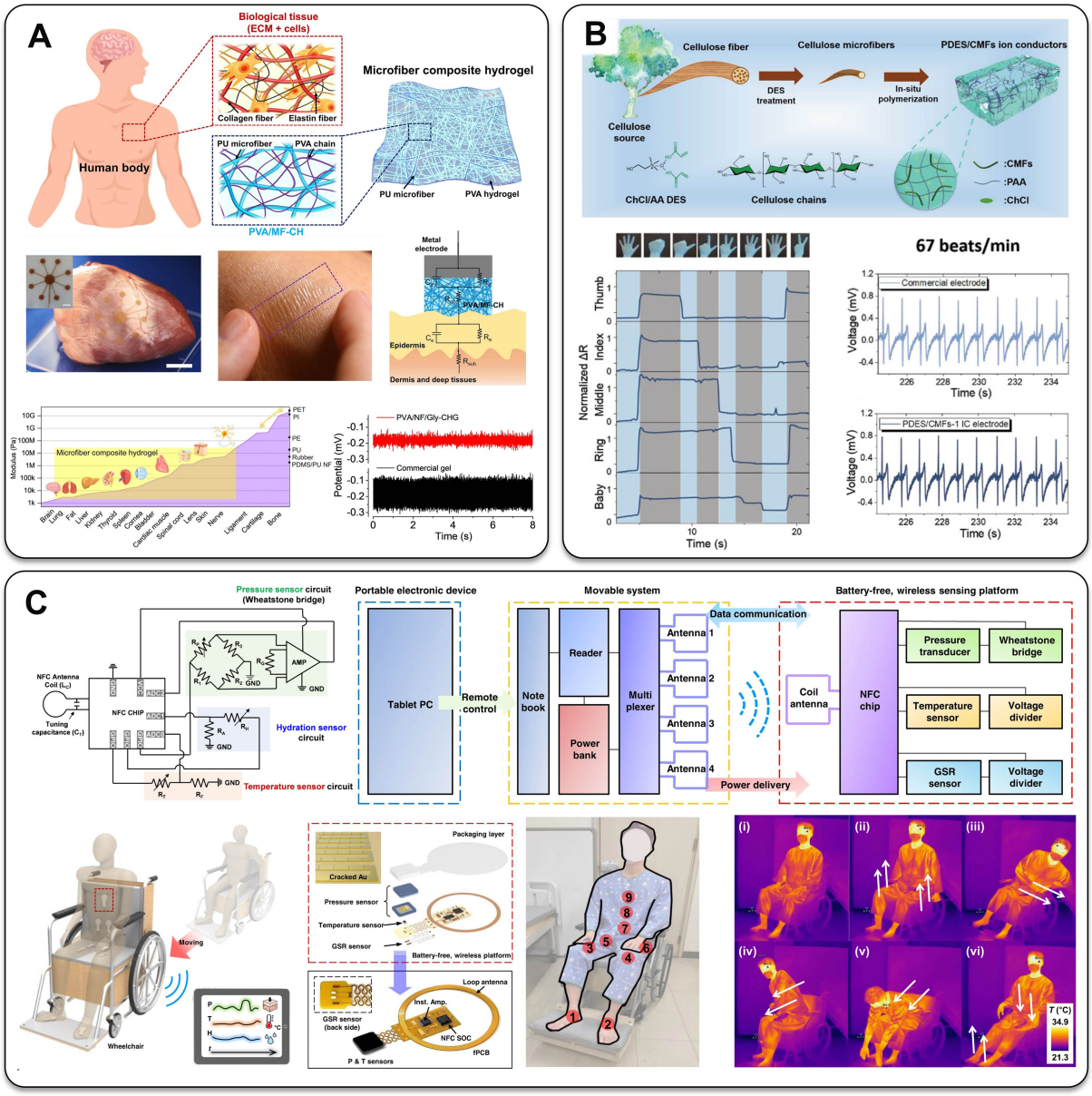

Figure 13. (A) schematic diagram of the microstructure, high mechanical adaptability to organs, and detection of EMG biological signals of PVA/MF/Gly-CH[215]; (B) schematic diagram of the preparation process, gesture detection, and detection of ECG signals of the PDES/CMFs flexible electrodes[216]; (C) schematic diagram of the architecture, composition and working process of the wireless electronic skin clinical detection system[217]. PU: Polyurethane; PVA: polyvinyl alcohol; MF-CH: microfiber composite hydrogel; PET: polyethylene terephthalate; PI: polyimide; PDMS: polydimethylsiloxane; NF: nanofiber; CMFs: cellulose microfibers; AMP: alkalized MXenes/polydopamine; EMG: electromyogram; MF: microfiber; ECG: electrocardiogram.

from this PDES/CMFs material proved its great potential for human motion sensing and physiological signal detection [Figure 13B].

As shown in Figure 13C, Cho *et al.* reported an e-skin system consisting of a multimodal sensor system and a wireless detection system (using the RF430FRL152H NFC SoC chip from Texas Instruments) for continuously monitoring pressure, temperature, and hydration at skin interfaces of a patient in a wheelchair[217]. The multimodal sensor system includes a pressure sensor, a temperature sensor, and a

galvanic skin response sensor. The wireless detection system communicates data with a plurality of wireless devices mounted on the skin of the wheelchair user, enabling accurate and stable measurements of pressure, temperature and hydration. Clinical trials with wheelchair patients demonstrated the feasibility and stability of the monolithic integrated system in preventing injuries caused by sedentary behavior.

Intelligent machinery

E-skins also possess vast potential in the field of intelligent machinery[218,219]. The application of e-skins in this area mainly includes two major aspects: remote control and mechanical haptics. For the former, the basic implementation method is to use e-skins as convenient signal sources and realize the convenient control of machinery by decoding the characteristics of the signals. Some scholars installed e-skins at the joint positions of hands or gloves and achieved synchronized control of a robotic hand by decoding the characteristic information transmitted by these e-skins in real time[220]. For the latter, the basic strategy is to install e-skins on the surface of the machinery so as to give the machinery tactile ability[221-223][Figure 14A (i) and Figure 14B (i)][224-229].

Zhang *et al.* designed a textile resistive pressure sensor, SPRET, consisting of a CNT network (conductive layer) + polypyrrole-polydopamine-perfluorodecyltrlethoxysilane (PPy-PDA-PFDS) polymer layer (hydrophobic layer) + a textile (substrate), exhibiting sparing to various reagents and high robustness[224]. This wearable e-skin can accurately, continuously, long-term and reliably detect human motion and physiological signals in air/humid conditions or underwater and also enable synchronized remote control of manipulators through a MCU [Figure 14A (i)].

Lu *et al.* developed hydroxypropyl cellulose (HPC)-based eutectic gels with high conductivity, transparency, and anti-freezing properties with 98.1% resilience suitable for wearable applications by introducing HPC into a metal salt-based deep eutectic solvent (MDES)[225]. Self-powered e-skin composed of this Eutectic Gel-Based Triboelectric Nanogenerator (E-TENG) prepared using this eutectic gel possesses excellent performance. Realized by an Arduino nano MCU (using ATmega328P Chip) for gesture recognition and robotic remote control, this highly resilient self-powered e-skin exhibits extraordinary potential for practical HMI and cooperative operation of intelligent machinery [Figure 14A (ii)].

Liu *et al.* proposed a capacitive bimodal e-skin, silicone rubber/4-Methylbenzenesulfonhydrazide/Silok-7455 Hyperdispersant/Polyphenylmethylsiloxane (SR/TSH/dispersant/PPMS), with 12 labyrinth-patterned sensing units in a pyramidal porous multistage dielectric structure for proximity and pressure sensing in HMI scenarios, which has a proximity detection range of 0-110 mm and a pressure detection range of 0-200 kPa, with a sensitivity of 0.464% kPa^{-1}[226]. The e-skin was used as a "keyboard" to enable real-time control of a robot arm through non-contact gestures and contact presses [Figure 14A (iii)].

Yang *et al.* report a self-healing high-performance flexible pressure sensor with MXene/PU (Sensitive Layer) - MXene (interdigital electrode) that can be prepared by a low-cost spraying method, which can be prepared on other arbitrary flexible substrates, with the hydrogen bonding of PU conferring self-healing functionality to the device[228]. The sensor exhibits high sensitivity (up to 509.8 kPa^{-1}) and good stability (10,000 cycles). This pressure sensor-based e-skin can be mounted on a robotic hand to give it haptic capabilities [Figure 14B (ii)].

Luo *et al.* demonstrated a capacitive-dielectric integrated pressure sensor, micro-conformal electrode-dielectric integration (MEDI), which has a complex structure of graphene nanowalls (pyramid-shaped top electrode)/PDMS (pyramid-shaped dielectric layer)/ZnO (pyramid-shaped dielectric layer)/poly(methyl

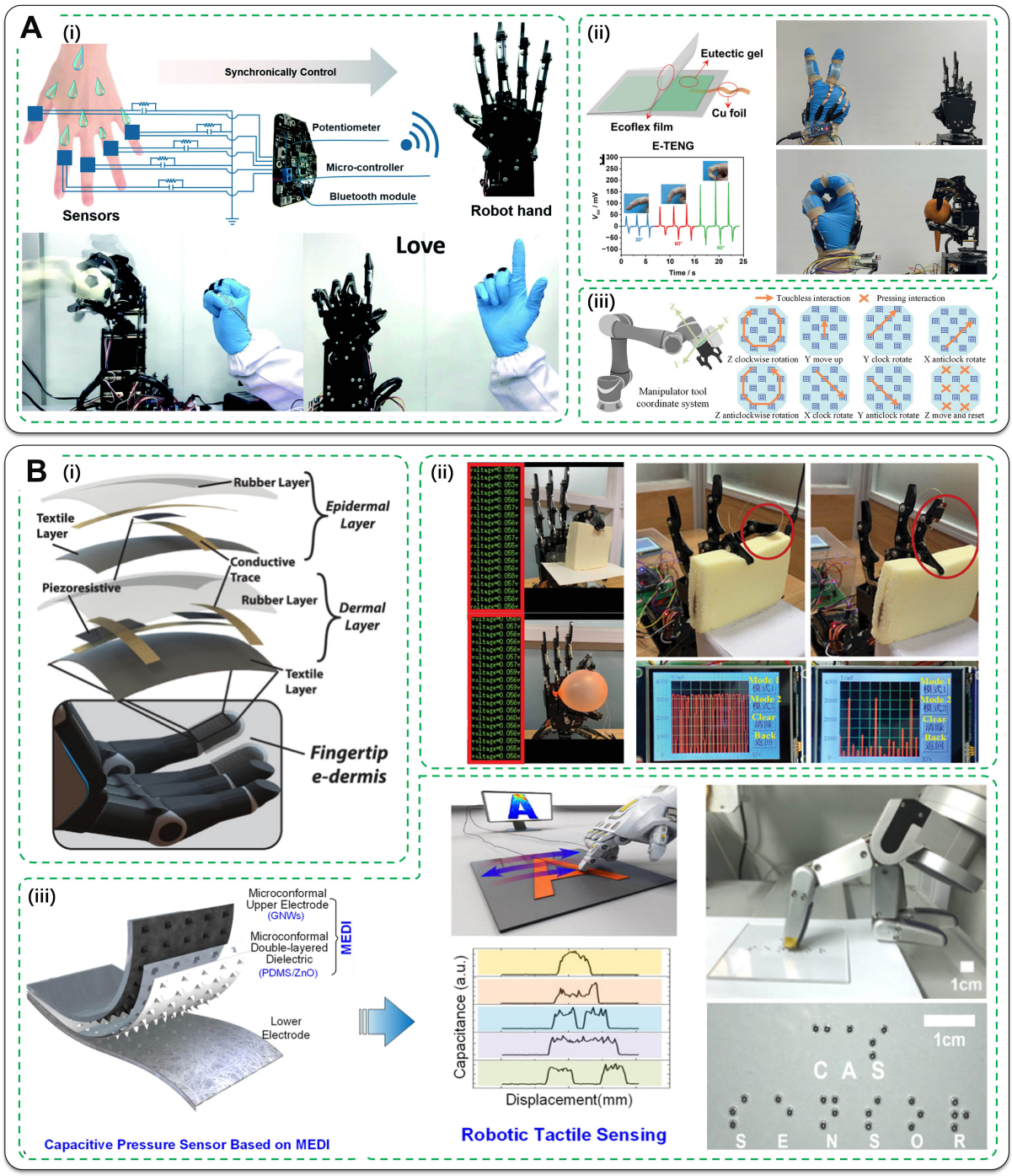

Figure 14. (A) Schematic diagram of remote control: (i) system composition and demonstration of synchronous control of SPRET e-skin[224], (ii) structure, sensing characteristics and synchronization control of e-skin based on E-TENG[225], (iii) demonstration of remote control of a robotic arm using the SR/TSH/dispersant/PPMS e-skin[226]; (B) Schematic diagram of mechanical tactility: (i) concept of mechanical tactile[227], (ii) demonstration of mechanical haptics of MXene/PU-MXene e-skin[228], (iii) mechanical haptic signals and its recognition of braille text of MEDI e-skin[229]. E-TENG: Eutectic Gel-Based Triboelectric Nanogenerator; GNWs: graphene nanowalls; PDMS: polydimethylsiloxane; MEDI: micro-conformal electrode-dielectric integration.

methacrylate) (PMMA, protective layer/dielectric layer)/AgNWs (bottom electrode)/polyethylene terephthalate (PET) (substrate)[228,229]. The introduction of the dielectric layer can effectively improve the

sensitivity (up to 22.3 kPa^{-1}) and pressure response range (0-22 kPa). Subsequently, the research team mounted it on a robotic hand to realize intelligent mechanical applications such as braille recognition, object grasping and roughness detection [Figure 14B (iii)].

PROSPECTS AND OUTLOOKS

In this review, we introduced the background and development of e-skins and outline the general strategies of various types of e-skins for realizing different basic functions, along with the latest advances in integrating these multiple functions into e-skin systems. We are pleased to see that the field of e-skins has been showing rapid development and making great strides every year, and we consider that the following trends will follow in the next period of time:

1. A major challenge remains how to integrate the various sensing characteristics better. This involves two key points: (1) the preparation of multimodal e-skins that integrate diverse powerful sensing capabilities; (2) the sensing characteristics are as non-interfering with each other as possible.

2. ML technologies will be applied in large numbers, accelerating the intelligent development of e-skins.

3. E-skins with special capabilities will increasingly emerge, expanding the applications of e-skins. For example, e-skins with good biocompatibility and degradability[230-232], suitable for medical and bioelectronic applications; e-skins having high transparency[159,233], suitable for photovoltaic and display applications. In fact, there have been e-skins with special capabilities such as light-emitting[234-236], thermal management[200], hydrophobicity[237,238], UV resistance[239], electromagnetic radiation resistance[200,240], and fire alarm[241].

4. Realizing these trends necessitates sophisticated designs in materials, circuits, processes, and signal processing. This calls for deep interdisciplinary collaboration among scientists in various fields such as chemistry, materials, mechatronics, electronics, information, and computers. For example, to achieve high performance, new high-performance sensors need to be designed from the material design, device structure design and other aspects, which requires the cooperation of scientists in the fields of chemistry, materials, mechanics, and so on. The trend of cross-field cooperation is more obvious in developing complex e-skin systems. The Multimodal E-skin Systems listed in the paper require fine design from chemistry, materials, mechanics, electronics, *etc*. to combine high performance and high reliability, and the IoT-Integrated and ML-Enabled E-skin Systems listed in the article involve a large number of technologies in the fields of electronics, information science, and computers. The applications of e-skins also require the contributions of multiple disciplines, such as medicine, biology, materials, chemistry, mechanics, electronics, and information technology, to be realized. And for the application of e-skin in other lesser-known fields, it is even more important to have cross-disciplinary collaboration to help inspire, promote, and apply. It is clear that these high-level, cutting-edge visions cannot be easily realized by traditional chemical and materials scientists alone and that cross-disciplinary research is the order of the day.

5. The signal communication in e-skin systems needs to be reformed. For example, for the synchronized remote control, which can be foreseen that such scenarios will inevitably become increasingly prevalent in the future, low latency is necessary, which means the requirements for fine material and structural design to improve the response speed, interface impedance, and other characteristics of the new e-skins[242,243].

6. Brain-computer interface (BCI) technology has made breakthroughs one after another in recent years[244,245]. In fact, it is a further in-depth development of the HMI concept, and it is foreseeable that e-skin will gain a lot of applications in this field. Similar to healthcare applications, but furthermore, the

requirements for non-toxicity and biocompatibility are more demanding, so we believe that some hydrogel materials with superior biocompatibility will be more suitable for applications in this field. On the other hand, it is clear that this is an extremely complex field that relies on the intimate cooperation of many disciplines such as biology, neurology, medicine, materials science, information science, ethics, mechanics, and so on.

DECLARATIONS

Authors' contributions

Determined the content and structure of the manuscript: Pang J, He P
Review and revise the manuscript: Li Z, Zhang S
Researching the literature and writing the manuscript: Zhu P
All authors have read the manuscript and approved the final version.

Availability of data and materials

Not applicable.

Financial support and sponsorship

The authors acknowledge the financial support from the National Natural Science Foundation of China (No. 52375327) and the Heilongjiang Provincial Natural Science Foundation of China (No. YQ2022E024).

Conflicts of interest

All authors declared that there are no conflicts of interest.

Ethical approval and consent to participate

Figures 3C, 4D, 5A, 5B, 6C, 12A, 12C, 13A, 13C and 14A are cited from the researches in refs.[62,72,82,83,95,199,200,215,217,224,225], respectively, showing partial body parts of the participants in the experiment. The purpose of these citations is to present the relevant research results and experimental methods more intuitively. The original images have been rigorously reviewed during the production of relevant illustrations to ensure the protection of the privacy of the experimental participants.

Consent for publication

Figures 5A, 5B, and 6C are cited from the researches in refs.[82,83,95], respectively, showing faces of the participants in the experiment. The original images have been rigorously reviewed during the production of relevant illustrations to ensure the protection of the privacy of the experimental participants.

REFERENCES

1. Lumelsky VJ, Shur MS, Wagner S. Sensitive skin. *IEEE Sens J* 2001;1:41-51. DOI
2. Abraira VE, Ginty DD. The sensory neurons of touch. *Neuron* 2013;79:618-39. DOI PubMed PMC
3. Amjadi M, Kyung K, Park I, Sitti M. Stretchable, skin-mountable, and wearable strain sensors and their potential applications: a review. *Adv Funct Mater* 2016;26:1678-98. DOI
4. Wang Y, Zhu P, Tan M, Niu M, Liang S, Mao Y. Recent advances in hydrogel-based self-powered artificial skins for human-machine interfaces. *Adv Intell Syst* 2023;5:2300162. DOI
5. Heng W, Solomon S, Gao W. Flexible electronics and devices as human-machine interfaces for medical robotics. *Adv Mater* 2022;34:e2107902. DOI PubMed PMC
6. Schwartz G, Tee BC, Mei J, et al. Flexible polymer transistors with high pressure sensitivity for application in electronic skin and health monitoring. *Nat Commun* 2013;4:1859. DOI
7. Yao S, Ren P, Song R, et al. Nanomaterial-enabled flexible and stretchable sensing systems: processing, integration, and applications. *Adv Mater* 2020;32:e1902343. DOI PubMed
8. Takei K, Takahashi T, Ho JC, et al. Nanowire active-matrix circuitry for low-voltage macroscale artificial skin. *Nat Mater* 2010;9:821-6. DOI

9. Xu X, Guo L, Liu H, et al. Stretchable electronic facial masks for skin electroporation. *Adv Funct Mater* 2024;34:2311144. DOI
10. Ye Y, Wan Z, Gunawardane PDSH, et al. Ultra-stretchable and environmentally resilient hydrogels via sugaring-out strategy for soft robotics sensing. *Adv Funct Mater* 2024:2315184. DOI
11. Ye Y, Oguzlu H, Zhu J, et al. Ultrastretchable ionogel with extreme environmental resilience through controlled hydration interactions. *Adv Funct Mater* 2023;33:2209787. DOI
12. Zhu P, Yu Z, Sun H, et al. 3D printed cellulose nanofiber aerogel scaffold with hierarchical porous structures for fast solar-driven atmospheric water harvesting. *Adv Mater* 2024;36:e2306653. DOI
13. Chen F, Zhang S, Hu L, et al. Bio-inspired artificial perceptual devices for neuromorphic computing and gesture recognition. *Adv Funct Mater* 2023;33:2300266. DOI
14. Zhan P, Zhai W, Wei W, et al. Stretchable strain sensor with high sensitivity, large workable range and excellent breathability for wearable electronic skins. *Compos Sci Technol* 2022;229:109720. DOI
15. Bi Y, Sun M, Zhang Y, et al. Seconds timescale synthesis of highly stretchable antibacterial hydrogel for skin wound closure and epidermal strain sensor. *Adv Healthc Mater* 2024;13:e2302810. DOI PubMed
16. Roy S, Deo KA, Lee HP, et al. 3D printed electronic skin for strain, pressure and temperature sensing. *Adv Funct Mater* 2024:2313575. DOI
17. Jiang N, Chang X, Hu D, et al. Flexible, transparent, and antibacterial ionogels toward highly sensitive strain and temperature sensors. *Chem Eng J* 2021;424:130418. DOI
18. Wu Z, Tai G, Liu R, Shao W, Hou C, Liang X. Synthesis of borophene on quartz towards hydroelectric generators. *J Mater Chem A* 2022;10:8218-26. DOI
19. Wang Y, Zhang L, Zhou J, Lu A. Flexible and transparent cellulose-based ionic film as a humidity sensor. *ACS Appl Mater Interfaces* 2020;12:7631-8. DOI
20. Shen D, Xiao M, Xiao Y, et al. Self-powered, rapid-response, and highly flexible humidity sensors based on moisture-dependent voltage generation. *ACS Appl Mater Interfaces* 2019;11:14249-55. DOI
21. Dai J, Zhao H, Lin X, et al. Ultrafast response polyelectrolyte humidity sensor for respiration monitoring. *ACS Appl Mater Interfaces* 2019;11:6483-90. DOI
22. Wang Y, Shu R, Zhang X. Strong, supertough and self-healing biomimetic layered nanocomposites enabled by reversible interfacial polymer chain sliding. *Angew Chem Int Ed Engl* 2023;62:e202303446. DOI PubMed
23. Pei D, Yu S, Liu P, et al. Reversible wet-adhesive and self-healing conductive composite elastomer of liquid metal. *Adv Funct Mater* 2022;32:2204257. DOI
24. Bunea AC, Dediu V, Laszlo EA, et al. E-skin: the dawn of a new era of on-body monitoring systems. *Micromachines* 2021;12:1091. DOI PubMed PMC
25. Hammock ML, Chortos A, Tee BC, Tok JB, Bao Z. 25th anniversary article: the evolution of electronic skin (e-skin): a brief history, design considerations, and recent progress. *Adv Mater* 2013;25:5997-6038. DOI PubMed
26. Yang JC, Mun J, Kwon SY, Park S, Bao Z, Park S. Electronic skin: recent progress and future prospects for skin-attachable devices for health monitoring, robotics, and prosthetics. *Adv Mater* 2019;31:e1904765. DOI PubMed
27. Chen J, Zhu Y, Chang X, et al. Recent progress in essential functions of soft electronic skin. *Adv Funct Mater* 2021;31:2104686. DOI
28. Li WD, Ke K, Jia J, et al. Recent advances in multiresponsive flexible sensors towards e-skin: a delicate design for versatile sensing. *Small* 2022;18:e2103734. DOI PubMed
29. Jung S, Kim JH, Kim J, et al. Reverse-micelle-induced porous pressure-sensitive rubber for wearable human-machine interfaces. *Adv Mater* 2014;26:4825-30. DOI PubMed
30. Lee Y, Myoung J, Cho S, et al. Bioinspired gradient conductivity and stiffness for ultrasensitive electronic skins. *ACS Nano* 2021;15:1795-804. DOI
31. Hou C, Wang H, Zhang Q, Li Y, Zhu M. Highly conductive, flexible, and compressible all-graphene passive electronic skin for sensing human touch. *Adv Mater* 2014;26:5018-24. DOI PubMed
32. Cai Y, Shen J, Yang CW, et al. Mixed-dimensional MXene-hydrogel heterostructures for electronic skin sensors with ultrabroad working range. *Sci Adv* 2020;6:eabb5367. DOI PubMed PMC
33. Sharma S, Chhetry A, Sharifuzzaman M, Yoon H, Park JY. Wearable capacitive pressure sensor based on MXene composite nanofibrous scaffolds for reliable human physiological signal acquisition. *ACS Appl Mater Interfaces* 2020;12:22212-24. DOI PubMed
34. Meng K, Xiao X, Wei W, et al. Wearable pressure sensors for pulse wave monitoring. *Adv Mater* 2022;34:e2109357. DOI PubMed
35. Claver U, Zhao G. Recent progress in flexible pressure sensors based electronic skin. *Adv Eng Mater* 2021;23:2001187. DOI
36. Zhang S, Li S, Xia Z, Cai K. A review of electronic skin: soft electronics and sensors for human health. *J Mater Chem B* 2020;8:852-62. DOI
37. Zhang J, Wei S, Liu C, et al. Porous nanocomposites with enhanced intrinsic piezoresistive sensitivity for bioinspired multimodal tactile sensors. *Microsyst Nanoeng* 2024;10:19. DOI PubMed PMC
38. Duan L, Spoerk M, Wieme T, et al. Designing formulation variables of extrusion-based manufacturing of carbon black conductive polymer composites for piezoresistive sensing. *Compos Sci Technol* 2019;171:78-85. DOI
39. Ding Y, Xu T, Onyilagha O, Fong H, Zhu Z. Recent advances in flexible and wearable pressure sensors based on piezoresistive 3D

monolithic conductive sponges. *ACS Appl Mater Interfaces* 2019;11:6685-704. DOI PubMed

40. Zheng S, Wu X, Huang Y, et al. Multifunctional and highly sensitive piezoresistive sensing textile based on a hierarchical architecture. *Compos Sci Technol* 2020;197:108255. DOI
41. Li K, Yang W, Yi M, Shen Z. Graphene-based pressure sensor and strain sensor for detecting human activities. *Smart Mater Struct* 2021;30:085027. DOI
42. Zhai Y, Yu Y, Zhou K, et al. Flexible and wearable carbon black/thermoplastic polyurethane foam with a pinnate-veined aligned porous structure for multifunctional piezoresistive sensors. *Chem Eng J* 2020;382:122985. DOI
43. Zheng Y, Xu H, Lou Z, Wang L, Han W. Ti_3C_2Tx quantum dots/leaf veins based sensors with ultra-broadrange high sensitivity. *J Phys D Appl Phys* 2023;56:485402. DOI
44. Oh J, Kim JO, Kim Y, et al. Highly uniform and low hysteresis piezoresistive pressure sensors based on chemical grafting of polypyrrole on elastomer template with uniform pore size. *Small* 2019;15:e1901744. DOI PubMed
45. Sencadas V, Tawk C, Alici G. Environmentally friendly and biodegradable ultrasensitive piezoresistive sensors for wearable electronics applications. *ACS Appl Mater Interfaces* 2020;12:8761-72. DOI PubMed
46. Park J, Lee Y, Hong J, et al. Tactile-direction-sensitive and stretchable electronic skins based on human-skin-inspired interlocked microstructures. *ACS Nano* 2014;8:12020-9. DOI
47. Park J, Lee Y, Hong J, et al. Giant tunneling piezoresistance of composite elastomers with interlocked microdome arrays for ultrasensitive and multimodal electronic skins. *ACS Nano* 2014;8:4689-97. DOI
48. Ha M, Lim S, Park J, Um D, Lee Y, Ko H. Bioinspired interlocked and hierarchical design of ZnO nanowire arrays for static and dynamic pressure-sensitive electronic skins. *Adv Funct Mater* 2015;25:2841-9. DOI
49. Miao L, Wan J, Song Y, et al. Skin-inspired humidity and pressure sensor with a wrinkle-on-sponge structure. *ACS Appl Mater Interfaces* 2019;11:39219-27. DOI
50. Park J, Kim J, Hong J, et al. Tailoring force sensitivity and selectivity by microstructure engineering of multidirectional electronic skins. *NPG Asia Mater* 2018;10:163-76. DOI
51. Baek J, Shan Y, Mylvaganan M, et al. Mold-free manufacturing of highly sensitive and fast-response pressure sensors through high-resolution 3D printing and conformal oxidative chemical vapor deposition polymers. *Adv Mater* 2023;35:e2304070. DOI PubMed
52. Mishra RB, El-Atab N, Hussain AM, Hussain MM. Flexible capacitive pressure sensors: recent progress on flexible capacitive pressure sensors: from design and materials to applications (Adv. Mater. Technol. 4/2021). *Adv Mater Technol* 2021;6:2001023. DOI
53. Wang H, Li Z, Liu Z, et al. Flexible capacitive pressure sensors for wearable electronics. *J Mater Chem C* 2022;10:1594-605. DOI
54. Lee J, Kwon H, Seo J, et al. Conductive fiber-based ultrasensitive textile pressure sensor for wearable electronics. *Adv Mater* 2015;27:2433-9. DOI PubMed
55. Lipomi DJ, Vosgueritchian M, Tee BC, et al. Skin-like pressure and strain sensors based on transparent elastic films of carbon nanotubes. *Nat Nanotechnol* 2011;6:788-92. DOI
56. Li J, Li J, Tang Y, et al. Touchable gustation via a hoffmeister gel iontronic sensor. *ACS Nano* 2023;17:5129-39. DOI
57. Chen W, Yan X. Progress in achieving high-performance piezoresistive and capacitive flexible pressure sensors: a review. *J MaterSci Technol* 2020;43:175-88. DOI
58. Kang S, Lee J, Lee S, et al. Highly sensitive pressure sensor based on bioinspired porous structure for real-time tactile sensing. *Adv Elect Mater* 2016;2:1600356. DOI
59. Tee BC, Chortos A, Dunn RR, Schwartz G, Eason E, Bao Z. Tunable flexible pressure sensors using microstructured elastomer geometries for intuitive electronics. *Adv Funct Mater* 2014;24:5427-34. DOI
60. Niu H, Gao S, Yue W, Li Y, Zhou W, Liu H. Highly morphology-controllable and highly sensitive capacitive tactile sensor based on epidermis-dermis-inspired interlocked asymmetric-nanocone arrays for detection of tiny pressure. *Small* 2020;16:e1904774. DOI PubMed
61. Yao G, Xu L, Cheng X, et al. Bioinspired triboelectric nanogenerators as self-powered electronic skin for robotic tactile sensing. *Adv Funct Mater* 2020;30:1907312. DOI
62. Zhu M, Lou M, Abdalla I, Yu J, Li Z, Ding B. Highly shape adaptive fiber based electronic skin for sensitive joint motion monitoring and tactile sensing. *Nano Energy* 2020;69:104429. DOI
63. Chen Y, Gao Z, Zhang F, Wen Z, Sun X. Recent progress in self-powered multifunctional e-skin for advanced applications. *Exploration* 2022;2:20210112. DOI PubMed PMC
64. Meng X, Cai C, Luo B, et al. Rational design of cellulosic triboelectric materials for self-powered wearable electronics. *Nanomicro Lett* 2023;15:124. DOI PubMed PMC
65. Wu M, Yao K, Li D, et al. Self-powered skin electronics for energy harvesting and healthcare monitoring. *Mater Today Energy* 2021;21:100786. DOI
66. Jiang Y, Dong K, Li X, et al. Stretchable, washable, and ultrathin triboelectric nanogenerators as skin-like highly sensitive self-powered haptic sensors. *Adv Funct Mater* 2021;31:2005584. DOI
67. Ma M, Zhang Z, Zhao Z, et al. Self-powered flexible antibacterial tactile sensor based on triboelectric-piezoelectric-pyroelectric multi-effect coupling mechanism. *Nano Energy* 2019;66:104105. DOI
68. Kwon SH, Zhang C, Jiang Z, Dong L. Textured nanofibers inspired by nature for harvesting biomechanical energy and sensing biophysiological signals. *Nano Energy* 2024;122:109334. DOI
69. Yu Y, Zhao X, Ge H, Ye L. A self-powered piezoelectric Poly(vinyl alcohol)/Polyvinylidene fluoride fiber membrane with

alternating multilayer porous structure for energy harvesting and wearable sensors. *Compos Sci Technol* 2024;247:110429. DOI
70. Scheffler S, Poulin P. Piezoelectric fibers: processing and challenges. *ACS Appl Mater Interfaces* 2022;14:16961-82. DOI PubMed
71. Ghosh SK, Mandal D. Synergistically enhanced piezoelectric output in highly aligned 1D polymer nanofibers integrated all-fiber nanogenerator for wearable nano-tactile sensor. *Nano Energy* 2018;53:245-57. DOI
72. Huang A, Zhu Y, Peng S, Tan B, Peng X. Improved energy harvesting ability of single-layer binary fiber nanocomposite membrane for multifunctional wearable hybrid piezoelectric and triboelectric nanogenerator and self-powered sensors. *ACS Nano* 2024;18:691-702. DOI
73. Du H, Zhou H, Wang M, et al. Electrospun elastic films containing AgNW-bridged MXene networks as capacitive electronic skins. *ACS Appl Mater Interfaces* 2022;14:31225-33. DOI
74. Wang H, Liu C, Li B, et al. Advances in carbon-based resistance strain sensors. *ACS Appl Electron Mater* 2023;5:674-89. DOI
75. Zhao Y, Liu Y, Li Y, Hao Q. Development and application of resistance strain force sensors. *Sensors* 2020;20:5826. DOI PubMed PMC
76. Chen J, Yu Q, Cui X, et al. An overview of stretchable strain sensors from conductive polymer nanocomposites. *J Mater Chem C* 2019;7:11710-30. DOI
77. Zhou M, Yu Y, Zhou Y, Song L, Wang S, Na D. Graphene-based strain sensor with sandwich structure and its application in bowel sounds monitoring. *RSC Adv* 2022;12:29103-12. DOI PubMed PMC
78. Feng P, Yuan Y, Zhong M, et al. Integrated resistive-capacitive strain sensors based on polymer-nanoparticle composites. *ACS Appl Nano Mater* 2020;3:4357-66. DOI
79. Chen J, Li H, Yu Q, et al. Strain sensing behaviors of stretchable conductive polymer composites loaded with different dimensional conductive fillers. *Compos Sci Technol* 2018;168:388-96. DOI
80. Ha S, Kim J. Simple route to performance modulation of resistive strain sensor based on strain-engineered stretchable substrate with customized hard template. *Compos Sci Technol* 2022;217:109111. DOI
81. Zhou Y, Zhan P, Ren M, et al. Significant stretchability enhancement of a crack-based strain sensor combined with high sensitivity and superior durability for motion monitoring. *ACS Appl Mater Interfaces* 2019;11:7405-14. DOI
82. Na HR, Lee HJ, Jeon JH, et al. Vertical graphene on flexible substrate, overcoming limits of crack-based resistive strain sensors. *npj Flex Electron* 2022;6:2. DOI
83. Qiao Y, Wang Y, Tian H, et al. Multilayer graphene epidermal electronic skin. *ACS Nano* 2018;12:8839-46. DOI
84. Chen Z, Yang Z, Yu T, et al. Sandwich-structured flexible PDMS@graphene multimodal sensors capable of strain and temperature monitoring with superlative temperature range and sensitivity. *Compos Sci Technol* 2023;232:109881. DOI
85. Fan M, Wu L, Hu Y, et al. A highly stretchable natural rubber/buckypaper/natural rubber (NR/N-BP/NR) sandwich strain sensor with ultrahigh sensitivity. *Adv Compos Hybrid Mater* 2021;4:1039-47. DOI
86. Han X, Xiao W, Wen S, et al. High-performance stretchable strain sensor based on Ag nanoparticles sandwiched between two 3D-printed polyurethane fibrous textiles. *Adv Elect Mater* 2021;7:2001242. DOI
87. Yang YF, Tao LQ, Pang Y, et al. An ultrasensitive strain sensor with a wide strain range based on graphene armour scales. *Nanoscale* 2018;10:11524-30. DOI
88. Kang D, Pikhitsa PV, Choi YW, et al. Ultrasensitive mechanical crack-based sensor inspired by the spider sensory system. *Nature* 2014;516:222-6. DOI
89. Chen Q, Chen K, Wu M, et al. Tough and fatigue-resistant anisotropic hydrogels via fiber reinforcement and magnetic field induction. *Sci China Mater* 2023;66:4841-52. DOI
90. Wang Q, Zhang Q, Wang G, Wang Y, Ren X, Gao G. Muscle-inspired anisotropic hydrogel strain sensors. *ACS Appl Mater Interfaces* 2022;14:1921-8. DOI
91. Chang X, Chen L, Chen J, Zhu Y, Guo Z. Advances in transparent and stretchable strain sensors. *Adv Compos Hybrid Mater* 2021;4:435-50. DOI
92. Lee CS, Hwang HS, Kim S, Fan J, Aghaloo T, Lee M. Inspired by nature: facile design of nanoclay-organic hydrogel bone sealant with multifunctional properties for robust bone regeneration. *Adv Funct Mater* 2020;30:2003717. DOI PubMed PMC
93. Afewerki S, Edlund U. Unlocking the power of multicatalytic synergistic transformation: toward environmentally adaptable organohydrogel. *Adv Mater* 2024;36:e2306657. DOI PubMed
94. Xie J, Su F, Fan L, et al. Robust and stretchable $Ti_3C_2T_x$ MXene/PEI conductive composite dual-network hydrogels for ultrasensitive strain sensing. *Compos Part A Appl Sci Manuf* 2024;176:107833. DOI
95. Lei D, Xiao Y, Xi M, Jiang Y, Li Y. Thermochromic and conductive hydrogels with tunable temperature sensitivity for dual sensing of temperature and human motion. *J Mater Chem C* 2023;12:232-44. DOI
96. Zhang X, Rong Y, Li H, et al. High tensile properties, wide temperature tolerance, and DLP-printable eutectogels for microarrays wearable strain sensors. *Chem Eng J* 2024;481:149004. DOI
97. Kim J, Hwang GW, Song M, et al. A reversible, versatile skin-attached haptic interface platform with bioinspired interconnection architectures capable of resisting sweat and vibration. *Adv Funct Mater* 2024;34:2311167. DOI
98. Gao X, Wang X, Fan X. Highly sensitive flexible strain sensor based on microstructured biphasic hydrogels for human motion monitoring. *Front Mater Sci* 2023;17:230665. DOI
99. Lu Y, Qu X, Wang S, et al. Ultradurable, freeze-resistant, and healable MXene-based ionic gels for multi-functional electronic skin. *Nano Res* 2022;15:4421-30. DOI

100. Li T, Wang Y, Li S, Liu X, Sun J. Mechanically robust, elastic, and healable ionogels for highly sensitive ultra-durable ionic skins. *Adv Mater* 2020;32:e2002706. DOI
101. Mao Y, Wang L, Wu Z, et al. Thermochromic optical/electrical hydrated ionogel with anti-freezing and self-healing ability for multimodal sensor. *Compos Commun* 2023;44:101769. DOI
102. Chun S, Son W, Choi C, et al. Bioinspired hairy skin electronics for detecting the direction and incident angle of airflow. *ACS Appl Mater Interfaces* 2019;11:13608-15. DOI
103. Ji B, Zhou Q, Chen G, et al. *In situ* assembly of a wearable capacitive sensor with a spine-shaped dielectric for shear-pressure monitoring. *J Mater Chem C* 2020;8:15634-45. DOI
104. Pang C, Lee GY, Kim TI, et al. A flexible and highly sensitive strain-gauge sensor using reversible interlocking of nanofibres. *Nat Mater* 2012;11:795-801. DOI
105. Yu H, Guo H, Wang J, et al. Skin-inspired capacitive flexible tactile sensor with an asymmetric structure for detecting directional shear forces. *Adv Sci* 2024;11:e2305883. DOI PubMed PMC
106. Zhu Y, Li Y, Xie D, et al. High-performance flexible tactile sensor enabled by multi-contact mechanism for normal and shear force measurement. *Nano Energy* 2023;117:108862. DOI
107. Chen H, Song Y, Guo H, et al. Hybrid porous micro structured finger skin inspired self-powered electronic skin system for pressure sensing and sliding detection. *Nano Energy* 2018;51:496-503. DOI
108. Joh H, Lee SW, Seong M, Lee WS, Oh SJ. Engineering the charge transport of Ag nanocrystals for highly accurate, wearable temperature sensors through all-solution processes. *Small* 2017;13:1700247. DOI
109. Jeon J, Lee HB, Bao Z. Flexible wireless temperature sensors based on Ni microparticle-filled binary polymer composites. *Adv Mater* 2013;25:850-5. DOI PubMed
110. Yamada S, Toshiyoshi H. Temperature sensor with a water-dissolvable ionic gel for ionic skin. *ACS Appl Mater Interfaces* 2020;12:36449-57. DOI PubMed
111. Ren X, Pei K, Peng B, et al. A low-operating-power and flexible active-matrix organic-transistor temperature-sensor array. *Adv Mater* 2016;28:4832-8. DOI PubMed
112. Tien NT, Jeon S, Kim DI, et al. A flexible bimodal sensor array for simultaneous sensing of pressure and temperature. *Adv Mater* 2014;26:796-804. DOI
113. Nag A, Simorangkir RB, Gawade DR, et al. Graphene-based wearable temperature sensors: a review. *Mater Design* 2022;221:110971. DOI
114. Liu R, He L, Cao M, Sun Z, Zhu R, Li Y. Flexible temperature sensors. *Front Chem* 2021;9:539678. DOI PubMed PMC
115. Wang L, Zhu R, Li G. Temperature and strain compensation for flexible sensors based on thermosensation. *ACS Appl Mater Interfaces* 2020;12:1953-61. DOI PubMed
116. Li Q, Zhang LN, Tao XM, Ding X. Review of flexible temperature sensing networks for wearable physiological monitoring. *Adv Healthc Mater* 2017;6:1601371. DOI PubMed
117. Li F, Xue H, Lin X, Zhao H, Zhang T. Wearable temperature sensor with high resolution for skin temperature monitoring. *ACS Appl Mater Interfaces* 2022;14:43844-52. DOI PubMed
118. Zhang C, Zhou Y, Han H, Zheng H, Xu W, Wang Z. Dopamine-triggered hydrogels with high transparency, self-adhesion, and thermoresponse as skinlike sensors. *ACS Nano* 2021;15:1785-94. DOI
119. Cao Z, Liu H, Jiang L. Transparent, mechanically robust, and ultrastable ionogels enabled by hydrogen bonding between elastomers and ionic liquids. *Mater Horiz* 2020;7:912-8. DOI
120. Li Z, Huang J, Zhou R, et al. Temperature decoupling of a hydrogel-based strain sensor under a dynamic temperature field. *Adv Mater Technol* 2023;8:2300404. DOI
121. Jia H, He Y, Zhang X, Du W, Wang Y. Integrating ultra-thermal-sensitive fluids into elastomers for multifunctional flexible sensors. *Adv Elect Mater* 2015;1:1500029. DOI
122. Ge G, Lu Y, Qu X, et al. Muscle-inspired self-healing hydrogels for strain and temperature sensor. *ACS Nano* 2020;14:218-28. DOI
123. Wang F, Chen J, Cui X, Liu X, Chang X, Zhu Y. Wearable ionogel-based fibers for strain sensors with ultrawide linear response and temperature sensors insensitive to strain. *ACS Appl Mater Interfaces* 2022;14:30268-78. DOI PubMed
124. Zhang M, Duan Z, Zhang B, et al. Electrochemical humidity sensor enabled self-powered wireless humidity detection system. *Nano Energy* 2023;115:108745. DOI
125. Gyu Son S, Jun Park H, Kim S, et al. Ultra-fast self-healable stretchable bio-based elastomer/graphene ink using fluid dynamics process for printed wearable sweat-monitoring sensor. *Chem Eng J* 2023;454:140443. DOI
126. Yin F, Guo Y, Qiu Z, et al. Hybrid electronic skin combining triboelectric nanogenerator and humidity sensor for contact and non-contact sensing. *Nano Energy* 2022;101:107541. DOI
127. Kano S, Kim K, Fujii M. Fast-response and flexible nanocrystal-based humidity sensor for monitoring human respiration and water evaporation on skin. *ACS Sens* 2017;2:828-33. DOI PubMed
128. Zhang D, Wang M, Tang M, et al. Recent progress of diversiform humidity sensors based on versatile nanomaterials and their prospective applications. *Nano Res* 2023;16:11938-58. DOI
129. Wang Y, Hou S, Li T, et al. Flexible capacitive humidity sensors based on ionic conductive wood-derived cellulose nanopapers. *ACS Appl Mater Interfaces* 2020;12:41896-904. DOI
130. Gu L, Zhou D, Cao JC. Piezoelectric active humidity sensors based on lead-free $NaNbO_3$ piezoelectric nanofibers. *Sensors*

2016;16:833. DOI PubMed PMC
131. Boudaden J, Steinmaßl M, Endres HE, et al. Polyimide-based capacitive humidity sensor. *Sensors* 2018;18:1516. DOI PubMed PMC
132. Hou C, Tai G, Liu Y, Wu Z, Wu Z, Liang X. Ultrasensitive humidity sensing and the multifunctional applications of borophene-MoS_2 heterostructures. *J Mater Chem A* 2021;9:13100-8. DOI
133. Liu X, Hou C, Liu Y, et al. Borophene and BC_2N quantum dot heterostructures: ultrasensitive humidity sensing and multifunctional applications. *J Mater Chem A* 2023;11:24789-99. DOI
134. Xu C, Zheng Z, Lin M, et al. Strengthened, antibacterial, and conductive flexible film for humidity and strain sensors. *ACS Appl Mater Interfaces* 2020;12:35482-92. DOI
135. Li T, Zhao T, Zhang H, et al. A skin-conformal and breathable humidity sensor for emotional mode recognition and non-contact human-machine interface. *npj Flex Electron* 2024;8:3. DOI
136. Chen L, Xu Y, Liu Y, et al. Flexible and transparent electronic skin sensor with sensing capabilities for pressure, temperature, and humidity. *ACS Appl Mater Interfaces* 2023;15:24923-32. DOI
137. Guo H, Lan C, Zhou Z, Sun P, Wei D, Li C. Transparent, flexible, and stretchable WS_2 based humidity sensors for electronic skin. *Nanoscale* 2017;9:6246-53. DOI
138. Duan Z, Yuan Z, Jiang Y, Yuan L, Tai H. Amorphous carbon material of daily carbon ink: emerging applications in pressure, strain, and humidity sensors. *J Mater Chem C* 2023;11:5585-600. DOI
139. Wang W, Nayeem MOG, Wang H, et al. Gas-permeable highly sensitive nanomesh humidity sensor for continuous measurement of skin humidity. *Adv Mater Technol* 2022;7:2200479. DOI
140. Jeong W, Song J, Bae J, Nandanapalli KR, Lee S. Breathable nanomesh humidity sensor for real-time skin humidity monitoring. *ACS Appl Mater Interfaces* 2019;11:44758-63. DOI
141. Li T, Li L, Sun H, et al. Porous ionic membrane based flexible humidity sensor and its multifunctional applications. *Adv Sci* 2017;4:1600404. DOI
142. Xu L, Zhai H, Chen X, et al. Coolmax/graphene-oxide functionalized textile humidity sensor with ultrafast response for human activities monitoring. *Chem Eng J* 2021;412:128639. DOI
143. Niu G, Wang Z, Xue Y, et al. Pencil-on-paper humidity sensor treated with nacl solution for health monitoring and skin characterization. *Nano Lett* 2023;23:1252-60. DOI
144. He J, Xiao P, Shi J, et al. High performance humidity fluctuation sensor for wearable devices via a bioinspired atomic-precise tunable graphene-polymer heterogeneous sensing junction. *Chem Mater* 2018;30:4343-54. DOI
145. Liu K, Wang M, Huang C, et al. Flexible bioinspired healable antibacterial electronics for intelligent human-machine interaction sensing. *Adv Sci* 2024;11:e2305672. DOI PubMed PMC
146. Wang Y, Huang X, Zhang X. Ultrarobust, tough and highly stretchable self-healing materials based on cartilage-inspired noncovalent assembly nanostructure. *Nat Commun* 2021;12:1291. DOI PubMed PMC
147. Khatib M, Zohar O, Saliba W, Haick H. A multifunctional electronic skin empowered with damage mapping and autonomic acceleration of self-healing in designated locations. *Adv Mater* 2020;32:e2000246. DOI PubMed
148. Jun S, Kim SO, Lee H, et al. Transparent, pressure-sensitive, and healable e-skin from a UV-cured polymer comprising dynamic urea bonds. *J Mater Chem A* 2019;7:3101-11. DOI
149. Liu R, Lai Y, Li S, et al. Ultrathin, transparent, and robust self-healing electronic skins for tactile and non-contact sensing. *Nano Energy* 2022;95:107056. DOI
150. Wang S, Urban MW. Self-healing polymers. *Nat Rev Mater* 2020;5:562-83. DOI
151. Huynh TP, Sonar P, Haick H. Advanced materials for use in soft self-healing devices. *Adv Mater* 2017:29. DOI PubMed
152. Han S, Chen S, Hu Z, et al. A near-infrared light-promoted self-healing photothermally conductive polycarbonate elastomer based on Prussian blue and liquid metal for sensors. *J Colloid Interface Sci* 2024;654:955-66. DOI
153. Yeh C, Lin C, Han T, Xiao Y, Chen Y, Chou H. Disulfide bond and Diels-Alder reaction bond hybrid polymers with high stretchability, transparency, recyclability, and intrinsic dual healability for skin-like tactile sensing. *J Mater Chem A* 2021;9:6109-16. DOI
154. Xun X, Zhang Z, Zhao X, et al. Highly robust and self-powered electronic skin based on tough conductive self-healing elastomer. *ACS Nano* 2020;14:9066-72. DOI
155. Gao Z, Lou Z, Han W, Shen G. A self-healable bifunctional electronic skin. *ACS Appl Mater Interfaces* 2020;12:24339-47. DOI
156. Zhang Z, Wang L, Yu H, et al. Highly transparent, self-healable, and adhesive organogels for bio-inspired intelligent ionic skins. *ACS Appl Mater Interfaces* 2020;12:15657-66. DOI
157. Wu J, Wu Z, Wei Y, et al. Ultrasensitive and stretchable temperature sensors based on thermally stable and self-healing organohydrogels. *ACS Appl Mater Interfaces* 2020;12:19069-79. DOI
158. Liao H, Guo X, Wan P, Yu G. Conductive MXene nanocomposite organohydrogel for flexible, healable, low-temperature tolerant strain sensors. *Adv Funct Mater* 2019;29:1904507. DOI
159. Liu J, Zhang L, Wang N, Zhao H, Li C. Nanofiber-reinforced transparent, tough, and self-healing substrate for an electronic skin with damage detection and program-controlled autonomic repair. *Nano Energy* 2022;96:107108. DOI
160. Wei P, Chen T, Chen G, et al. Conductive self-healing nanocomposite hydrogel skin sensors with antifreezing and thermoresponsive properties. *ACS Appl Mater Interfaces* 2020;12:3068-79. DOI

161. Chen X, Sun P, Tian H, et al. Self-healing and stretchable conductor based on embedded liquid metal patterns within imprintable dynamic covalent elastomer. *J Mater Chem C* 2022;10:1039-47. DOI
162. Wang S, Bi S, Zhang L, Liu R, Wang H, Gu J. Skin-inspired antibacterial conductive hydrogels customized for wireless flexible sensor and collaborative wound healing. *J Mater Chem A* 2023;11:14096-107. DOI
163. Pan X, Wang Q, Guo R, et al. An adaptive ionic skin with multiple stimulus responses and moist-electric generation ability. *J Mater Chem A* 2020;8:17498-506. DOI
164. Liu Z, Wang Y, Ren Y, et al. Poly(ionic liquid) hydrogel-based anti-freezing ionic skin for a soft robotic gripper. *Mater Horiz* 2020;7:919-27. DOI
165. Wang Y, Chang Q, Zhan R, et al. Tough but self-healing and 3D printable hydrogels for E-skin, E-noses and laser controlled actuators. *J Mater Chem A* 2019;7:24814-29. DOI
166. Cui X, Chen J, Zhu Y, Jiang W. Natural sunlight-actuated shape memory materials with reversible shape change and self-healing abilities based on carbon nanotubes filled conductive polymer composites. *Chem Eng J* 2020;382:122823. DOI
167. Son D, Kang J, Vardoulis O, et al. An integrated self-healable electronic skin system fabricated via dynamic reconstruction of a nanostructured conducting network. *Nat Nanotechnol* 2018;13:1057-65. DOI
168. Li Y, Chen S, Wu M, Sun J. Polyelectrolyte multilayers impart healability to highly electrically conductive films. *Adv Mater* 2012;24:4578-82. DOI
169. Zhao Z, Soni S, Lee T, Nijhuis CA, Xiang D. Smart eutectic gallium-indium: from properties to applications. *Adv Mater* 2023;35:e2203391. DOI PubMed
170. Chen S, Fan S, Chan H, et al. Liquid metal functionalization innovations in wearables and soft robotics for smart healthcare applications. *Adv Funct Mater* 2023:2309989. DOI
171. Xu C, Ma B, Yuan S, Zhao C, Liu H. High-resolution patterning of liquid metal on hydrogel for flexible, stretchable, and self-healing electronics. *Adv Elect Mater* 2020;6:1900721. DOI
172. Guo R, Sun X, Yuan B, Wang H, Liu J. Magnetic liquid metal (Fe-EGaIn) based multifunctional electronics for remote self-healing materials, degradable electronics, and thermal transfer printing. *Adv Sci* 2019;6:1901478. DOI PubMed PMC
173. Yun G, Tang SY, Sun S, et al. Liquid metal-filled magnetorheological elastomer with positive piezoconductivity. *Nat Commun* 2019;10:1300. DOI PubMed PMC
174. Markvicka EJ, Bartlett MD, Huang X, Majidi C. An autonomously electrically self-healing liquid metal-elastomer composite for robust soft-matter robotics and electronics. *Nat Mater* 2018;17:618-24. DOI PubMed
175. Wang M, Rojas OJ, Ning L, et al. Liquid metal and Mxene enable self-healing soft electronics based on double networks of bacterial cellulose hydrogels. *Carbohydr Polym* 2023;301:120330. DOI
176. Chu K, Song BG, Yang H, et al. Smart passivation materials with a liquid metal microcapsule as self-healing conductors for sustainable and flexible perovskite solar cells. *Adv Funct Mater* 2018;28:1800110. DOI
177. Blaiszik BJ, Kramer SL, Grady ME, et al. Autonomic restoration of electrical conductivity. *Adv Mater* 2012;24:398-401. DOI
178. Dickey MD, Chiechi RC, Larsen RJ, Weiss EA, Weitz DA, Whitesides GM. Eutectic gallium-indium (EGaIn): a liquid metal alloy for the formation of stable structures in microchannels at room temperature. *Adv Funct Mater* 2008;18:1097-104. DOI
179. Krisnadi F, Nguyen LL, Ankit, et al. Directed assembly of liquid metal-elastomer conductors for stretchable and self-healing electronics. *Adv Mater* 2020;32:e2001642. DOI
180. Park S, Thangavel G, Parida K, Li S, Lee PS. A stretchable and self-healing energy storage device based on mechanically and electrically restorative liquid-metal particles and carboxylated polyurethane composites. *Adv Mater* 2019;31:e1805536. DOI PubMed
181. Shi C, Zou Z, Lei Z, Zhu P, Zhang W, Xiao J. Heterogeneous integration of rigid, soft, and liquid materials for self-healable, recyclable, and reconfigurable wearable electronics. *Sci Adv* 2020;6:eabd0202. DOI PubMed PMC
182. Ren X, Song M, Jiang J, et al. Fire-retardant and thermal-insulating cellulose nanofibril aerogel modified by in situ supramolecular assembly of melamine and phytic acid. *Adv Eng Mater* 2022;24:2101534. DOI
183. Wang Y, Yue Y, Cheng F, et al. Ti_3C_2Tx MXene-based flexible piezoresistive physical sensors. *ACS Nano* 2022;16:1734-58. DOI
184. Sun X, Mao Y, Yu Z, Yang P, Jiang F. A biomimetic "salting out-alignment-locking" tactic to design strong and tough hydrogel. *Adv Mater* 2024:e2400084. DOI PubMed
185. Mu C, Wang Y, Mei D, Wang S. Development of robotic hand tactile sensing system for distributed contact force sensing in robotic dexterous multimodal grasping. *Int J Intell Robot Appl* 2022;6:760-72. DOI
186. Deng C, Tang W, Liu L, Chen B, Li M, Wang ZL. Self-powered insole plantar pressure mapping system. *Adv Funct Mater* 2018;28:1801606. DOI
187. Tu J, Wang M, Li W, et al. Electronic skins with multimodal sensing and perception. *Soft Sci* 2023;3:25. DOI
188. Jeon S, Lim S, Trung TQ, Jung M, Lee N. Flexible multimodal sensors for electronic skin: principle, materials, device, array architecture, and data acquisition method. *Proc IEEE* 2019;107:2065-83. DOI
189. Won SM, Wang H, Kim BH, et al. Multimodal sensing with a three-dimensional piezoresistive structure. *ACS Nano* 2019;13:10972-9. DOI
190. Wang C, Xia K, Zhang M, Jian M, Zhang Y. An all-silk-derived dual-mode e-skin for simultaneous temperature-pressure detection. *ACS Appl Mater Interfaces* 2017;9:39484-92. DOI PubMed
191. Lou Z, Chen S, Wang L, et al. Ultrasensitive and ultraflexible e-skins with dual functionalities for wearable electronics. *Nano Energy*

2017;38:28-35. DOI
192. Yang R, Zhang W, Tiwari N, Yan H, Li T, Cheng H. Multimodal sensors with decoupled sensing mechanisms. *Adv Sci* 2022;9:e2202470. DOI PubMed PMC
193. Peng S, Wu S, Yu Y, Xia B, Lovell NH, Wang CH. Multimodal capacitive and piezoresistive sensor for simultaneous measurement of multiple forces. *ACS Appl Mater Interfaces* 2020;12:22179-90. DOI
194. Ho DH, Sun Q, Kim SY, Han JT, Kim DH, Cho JH. Stretchable and multimodal all graphene electronic skin. *Adv Mater* 2016;28:2601-8. DOI PubMed
195. Zhao XF, Wen XH, Sun P, et al. Spider web-like flexible tactile sensor for pressure-strain simultaneous detection. *ACS Appl Mater Interfaces* 2021;13:10428-36. DOI
196. Hua Q, Sun J, Liu H, et al. Skin-inspired highly stretchable and conformable matrix networks for multifunctional sensing. *Nat Commun* 2018;9:244. DOI PubMed PMC
197. Lin W, Wang B, Peng G, Shan Y, Hu H, Yang Z. Skin-inspired piezoelectric tactile sensor array with crosstalk-free row+column electrodes for spatiotemporally distinguishing diverse stimuli. *Adv Sci* 2021;8:2002817. DOI PubMed PMC
198. Shin J, Jeong B, Kim J, et al. Sensitive wearable temperature sensor with seamless monolithic integration. *Adv Mater* 2020;32:e1905527. DOI PubMed
199. Zhang J, Hu Y, Zhang L, Zhou J, Lu A. Transparent, ultra-stretching, tough, adhesive carboxyethyl chitin/polyacrylamide hydrogel toward high-performance soft electronics. *Nanomicro Lett* 2022;15:8. DOI PubMed PMC
200. Wang X, Tao Y, Zhao C, et al. Bionic-leaf vein inspired breathable anti-impact wearable electronics with health monitoring, electromagnetic interference shielding and thermal management. *J Mater Sci Technol* 2024;188:216-27. DOI
201. Liu C, Zhao C, Wang Y, Wang H. Machine-learning-based calibration of temperature sensors. *Sensors* 2023;23:7347. DOI PubMed PMC
202. Wang M, Wang T, Luo Y, et al. Fusing stretchable sensing technology with machine learning for human-machine interfaces. *Adv Funct Mater* 2021;31:2008807. DOI
203. Xu C, Song Y, Sempionatto JR, et al. A physicochemical-sensing electronic skin for stress response monitoring. *Nat Electron* 2024;7:168-79. DOI PubMed PMC
204. Pyun KR, Kwon K, Yoo MJ, et al. Machine-learned wearable sensors for real-time hand-motion recognition: toward practical applications. *Natl Sci Rev* 2024;11:nwad298. DOI PubMed PMC
205. Xu C, Solomon SA, Gao W. Artificial intelligence-powered electronic skin. *Nat Mach Intell* 2023;5:1344-55. DOI PubMed PMC
206. Huang Q, Jiang Y, Duan Z, et al. Electrochemical self-powered strain sensor for static and dynamic strain detections. *Nano Energy* 2023;118:108997. DOI
207. Dawar N, Kehtarnavaz N. Action detection and recognition in continuous action streams by deep learning-based sensing fusion. *IEEE Sensors J* 2018;18:9660-8. DOI
208. Shen L, Liu M, Lu L, et al. Domain-engineered flexible ferrite membrane for novel machine learning based multimodal flexible sensing. *Adv Mater Inter* 2022;9:2101989. DOI
209. Li N, Wang Z, Yang X, et al. Deep-learning-assisted thermogalvanic hydrogel e-skin for self-powered signature recognition and biometric authentication. *Adv Funct Mater* 2024;34:2314419. DOI
210. Wang L, Liu J, Qi X, et al. Personal protective gloves with objects recognizing for rescuing in disaster. *Chem Eng J* 2023;477:146986. DOI
211. Niu H, Li H, Zhang Q, Kim ES, Kim NY, Li Y. Intuition-and-tactile bimodal sensing based on artificial-intelligence-motivated all-fabric bionic electronic skin for intelligent material perception. *Small* 2024;20:e2308127. DOI PubMed
212. Kim KK, Ha I, Kim M, et al. A deep-learned skin sensor decoding the epicentral human motions. *Nat Commun* 2020;11:2149. DOI PubMed PMC
213. Tan H, Zhou Y, Tao Q, Rosen J, van Dijken S. Bioinspired multisensory neural network with crossmodal integration and recognition. *Nat Commun* 2021;12:1120. DOI PubMed PMC
214. Bai Z, Wang X, Zheng M, et al. Mechanically robust and transparent organohydrogel-based e-skin nanoengineered from natural skin. *Adv Funct Mater* 2023;33:2212856. DOI
215. Gao Q, Sun F, Li Y, et al. Biological tissue-inspired ultrasoft, ultrathin, and mechanically enhanced microfiber composite hydrogel for flexible bioelectronics. *Nanomicro Lett* 2023;15:139. DOI PubMed PMC
216. Sun X, Zhu Y, Zhu J, Le K, Servati P, Jiang F. Tough and ultrastretchable liquid-free ion conductor strengthened by deep eutectic solvent hydrolyzed cellulose microfibers. *Adv Funct Mater* 2022;32:2202533. DOI
217. Cho S, Han H, Park H, et al. Wireless, multimodal sensors for continuous measurement of pressure, temperature, and hydration of patients in wheelchair. *npj Flex Electron* 2023;7:8. DOI
218. Yin F, Niu H, Kim E, Shin YK, Li Y, Kim N. Advanced polymer materials-based electronic skins for tactile and non-contact sensing applications. *InfoMat* 2023;5:e12424. DOI
219. Beker L, Matsuhisa N, You I, et al. A bioinspired stretchable membrane-based compliance sensor. *Proc Natl Acad Sci U S A* 2020;117:11314-20. DOI PubMed PMC
220. Tao K, Chen Z, Yu J, et al. Ultra-sensitive, deformable, and transparent triboelectric tactile sensor based on micro-pyramid patterned ionic hydrogel for interactive human-machine interfaces. *Adv Sci* 2022;9:e2104168. DOI PubMed PMC
221. Boutry CM, Negre M, Jorda M, et al. A hierarchically patterned, bioinspired e-skin able to detect the direction of applied pressure for

robotics. *Sci Robot* 2018;3:eaau6914. DOI

222. Zhu L, Wang Y, Mei D, et al. Large-area hand-covering elastomeric electronic skin sensor with distributed multifunctional sensing capability. *Adv Intell Syst* 2022;4:2100118. DOI
223. Zhang C, Liu S, Huang X, Guo W, Li Y, Wu H. A stretchable dual-mode sensor array for multifunctional robotic electronic skin. *Nano Energy* 2019;62:164-70. DOI
224. Zhang L, He J, Liao Y, et al. A self-protective, reproducible textile sensor with high performance towards human-machine interactions. *J Mater Chem A* 2019;7:26631-40. DOI
225. Lu C, Wang X, Shen Y, et al. Skin-like transparent, high resilience, low hysteresis, fatigue-resistant cellulose-based eutectogel for self-powered e-skin and human-machine interaction. *Adv Funct Mater* 2024;34:2311502. DOI
226. Liu W, Xiang F, Mei D, Wang Y. A flexible dual-mode capacitive sensor for highly sensitive touchless and tactile sensing in human-machine interactions. *Adv Mater Technol* 2024;9:2301685. DOI
227. Osborn LE, Dragomir A, Betthauser JL, et al. Prosthesis with neuromorphic multilayered e-dermis perceives touch and pain. *Sci Robot* 2018;3:10. DOI PubMed PMC
228. Yang M, Cheng Y, Yue Y, et al. High-performance flexible pressure sensor with a self-healing function for tactile feedback. *Adv Sci* 2022;9:e2200507. DOI PubMed PMC
229. Luo S, Zhou X, Tang X, et al. Microconformal electrode-dielectric integration for flexible ultrasensitive robotic tactile sensing. *Nano Energy* 2021;80:105580. DOI
230. Yang JY, Kumar A, Shaikh MO, et al. Biocompatible, antibacterial, and stable deep eutectic solvent-based ionic gel multimodal sensors for healthcare applications. *ACS Appl Mater Interfaces* 2023;15:55244-57. DOI
231. Peng Z, Zhu C, Zhang X, Zhang L. Advancing the pressure sensing performance and biocompatible of conductive rGO/PEDOT/PDMS composite film for simple and efficient pressure sensor. *Smart Mater Struct* 2023;32:125020. DOI
232. Wan S, Zhu Z, Yin K, et al. A highly skin-conformal and biodegradable graphene-based strain sensor. *Small Methods* 2018;2:1700374. DOI
233. Wang Y, Zhang L, Lu A. Highly stretchable, transparent cellulose/PVA composite hydrogel for multiple sensing and triboelectric nanogenerators. *J Mater Chem A* 2020;8:13935-41. DOI
234. Wang C, Hwang D, Yu Z, et al. User-interactive electronic skin for instantaneous pressure visualization. *Nat Mater* 2013;12:899-904. DOI
235. Zhang Z, Wang Y, Jia S, Fan C. Body-conformable light-emitting materials and devices. *Nat Photon* 2024;18:114-26. DOI
236. Cheng Y, Li L, Meredith CH, et al. Photoluminescent humidity sensors based on droplet-enabled porous composite gels. *ACS Mater Lett* 2023;5:2074-83. DOI
237. Tan D, Xu B, Chung KY, et al. Self-adhesive, detach-on-demand, and waterproof hydrophobic electronic skins with customized functionality and wearability. *Adv Funct Mater* 2024;34:2311457. DOI
238. Lin J, Cai X, Liu Z, et al. Anti-liquid-interfering and bacterially antiadhesive strategy for highly stretchable and ultrasensitive strain sensors based on cassie-baxter wetting state. *Adv Funct Mater* 2020;30:2000398. DOI
239. Pan X, Wang Q, Guo R, et al. An integrated transparent, UV-filtering organohydrogel sensor *via* molecular-level ion conductive channels. *J Mater Chem A* 2019;7:4525-35. DOI
240. Cai J, Li J, Chen X, Wang M. Multifunctional polydimethylsiloxane foam with multi-walled carbon nanotube and thermo-expandable microsphere for temperature sensing, microwave shielding and piezoresistive sensor. *Chem Eng J* 2020;393:124805. DOI
241. Wei W, Yi Y, Song J, Chen X, Li J, Li J. Tunable graphene/nitrocellulose temperature alarm sensors. *ACS Appl Mater Interfaces* 2022;14:13790-800. DOI PubMed PMC
242. Tan D, Xu B. Advanced interfacial design for electronic skins with customizable functionalities and wearability. *Adv Funct Mater* 2023;33:2306793. DOI
243. Huang C, Chiu C. Facile fabrication of a stretchable and flexible nanofiber carbon film-sensing electrode by electrospinning and its application in smart clothing for ECG and EMG monitoring. *ACS Appl Electron Mater* 2021;3:676-86. DOI
244. Li C, Zhao W. Progress in the brain-computer interface: an interview with Bin He. *Natl Sci Rev* 2020;7:480-3. DOI PubMed PMC
245. Venkatesh, Kavya, Keerthi R, Ikshu B, Badarish IT. Neuralink and brain control machine. *IJARSCT* 2022;2. Available from: https://ijarsct.co.in/Paper3135.pdf. [Last accessed on 7 May 2024].